Environmental
Studies
Research
Fund

209

Quantitative Assessment of the Interaction between Beaufort Sea Crude Oils and Mackenzie River Delta Suspended Sediments

Évaluation quantitative de l’interaction entre des huiles brutes de la Mer de Beaufort et les sédiments en suspension du Delta du fleuve Mackenzie

March 2017

Quantitative Assessment of the Interaction between Beaufort Sea Crude Oils and Mackenzie River Delta Suspended Sediments

Évaluation quantitative de l'interaction entre des huiles brutes de la Mer de Beaufort et les sédiments en suspension du Delta du fleuve Mackenzie

ESRF Report 209

Prepared for:

Environmental Studies Research Funds Program (ESRF)

Submitted by

Dr. Ali Khelifa
Mr. Ben Fieldhouse
Dr. Carl E. Brown
Emergencies Science and Technology Section (ESTS)
Science and Technology Branch
Environment and Climate Change Canada
335 River Road
Ottawa, Ontario, K1A 0H3
Canada

March 14, 2017

Executive Summary

It is well established that aggregation between suspended oil droplets and suspended particulate matter (SPM), which leads to the formation of oil-SPM aggregates (OSAs), has strong control on the fate and behaviour of oil spills in coastal water rich in SPM. However, very limited (if any) research work has been conducted on this natural process for the Mackenzie River Delta in the Beaufort Sea and the Mackenzie River in Norman Wells water systems.

This project aimed to conduct an extensive laboratory study to establish a quantitative understanding of OSA formation using Arctic crude oils from the Beaufort Sea and Norman Wells, NWT and several natural sediments from the Mackenzie River Delta and Norman Wells. The names of these Arctic oils are Norman Wells, Amauligak and Atkinson.

In the first part of the project, oil dispersion and droplet formation were studied using different techniques. Substantial amount of new data on oil/brine interfacial tension (IFT) and size distribution of dispersed oil droplets was generated to support, among others, modelling of spills of the three oils under different conditions. At 5 ppt water salinity and no dispersant, IFT of Amauligak decreased from 22.5 to 21 mN/m when the temperature was increased from 0 to 30 ^{o}C. At 15 ^{o}C and no dispersant, IFT of Amauligak decreased from 23.1 to 22.3 when water salinity was increased from 0 to 33 ppt. When Corexit EC950A was applied, IFT reduces significantly. A small DOR of 1:500 causes a reduction of the IFT of Amauligak crude oil by about 18 mN/m (IFT decreases from 22.3 to 3.6 mN/m). This was observed at both 5 and 33 ppt water salinities.

In the second part of the project, findings showed that negatively buoyant OSAs form readily with the three Arctic crude oils using moderate mixing energy at 15 ^{o}C and freezing temperature of 0 ^{o}C. Application of Corexit EC9500A enhanced OSA formation, even at a small dispersant-to-oil ratio of 1:500. A key controlling factor for this OSA formation is fine content. Sediments rich in fines less than about 5 μm in size are superior candidates in forming OSAs.

Water salinity was shown to have a strong influence on OSA formation when increased from 0 to about 10 ppt. OSA formed at 33ppt have physical properties similar to sediment flocs. However, results showed that the presence of oil droplets in their structure enhance OSA resistance to shear due to the strong bonding between the sediment fines and oil droplets.

Sommaire

Il est bien établi que l'agrégation entre les gouttelettes suspendues d'huile de pétrole et les particules de matière en suspension (PMS), ce qui conduit à la formation d'agrégats pétrole-PMS (APPs), a une grande influence sur le comportement de déversements d'huile de pétrole dans les eaux côtières riches en PMS. Cependant, très peu de travaux de recherche ont été effectués sur ce mécanisme naturel pour les milieux aquatiques du delta de la rivière Mackenzie dans la mer du Beaufort et de la rivière Mackenzie à Norman Wells.

L'objectif principal de ce projet est d'effectuer une étude de laboratoire intensive afin d'établir des connaissances quantitatives sur la formation d'APPs en utilisant des huiles de pétrole bruts provenant de la mer de Beaufort et du Norman Wells. Le projet consiste aussi à utiliser des sédiments naturels provenant du delta de la rivière Mackenzie et de la rivière Mackenzie à Norman Wells.

Dans la première partie de ce projet, la dispersion d'huile et la formation de gouttelettes ont été étudiées en utilisant des techniques différentes. Un volume important de nouvelles données sur la tension superficielle (TS) et la distribution de taille des gouttelettes dispersées a été produit. Ces données sont fondamentales pour la modélisation de déversements des trois huiles sous des conditions différentes. A une salinité de 5 ppt et sans dispersant, la TS d'Amauligak décroit de 22.5 à 21 mN/m lorsque la température est augmentée de 0 à 30 ^{o}C. A une température de 15 oC et sans dispersant, la TS d'Amauligak décroit de 23.1 à 22.3 lorsque la salinité est augmentée de 0 à 33 ppt. Lorsque Corexit EC9500A est applique, la TS est démunie significativement. Une petite dose de 1 :500 de Corexit EC9500A a causée une réduction de la TS d'Amauligak par environ 18 mN/m (la TS est réduite de 22.3 à 3.6 mN/m). Ceci est observé à deux salinités de 5 et 33 ppt.

Dans la deuxième partie de ce projet, les résultats montrent que les APPs se forment facilement avec les trois huiles de pétroles bruts suivants provenant de l'Arctique: Norman Wells, Amauligak et Atkinson. Ceci en utilisant une énergie d'agitation modérée et deux températures de 15 et 0 ^{o}C. L'application du dispersant chimique Corexit EC9500A augmente la formation d'APPs, même avec un faible dosage de 1:500. Le paramètre clef contrôlant cette formation d'APPs est l'abondance des particules fines. En effet, les sédiments riches en particule fines plus petites d'environ 5 μm sont des candidats supérieurs pour la formation d'APPs.

La salinité des eaux avait une forte influence sur la formation des APPs lorsqu'elle augmentait de 0 à environ 10 ppt. Les APPs formées avec une eau de salinité de 33 ppt avaient des propriétés physiques similaires à ceux des flocs de sédiments. Cependant, les résultats montrent que la présence de gouttelettes d'huiles dans leurs structures augmente la résistance des APPs aux mouvements turbulents. Ceci est due à la solidité de l'agrégation entres les particules fines de sédiments et les gouttelettes d'huiles.

Acknowledgements

Funding for this project was provided by Environmental Studies Research Funds Program (ESRF) of Natural Resources Canada. The following researchers and students have made substantial contribution to this project. We would like to thank them all. We also would like to remind the reader that this work is ours and we are responsible for any mistakes, mis-interpretations or confusions that may contain.

Brian Yurris and **Ryan Lennie**, Water Survey of Canada, Environment and Climate Change Canada: Conducted extensive sediment sampling from the Mackenzie River in Norman Wells specifically for this project.

Dustin Whalen, Geological Survey of Canada, Natural Resources Canada: Conducted extensive sampling from the Mackernzie River Delta in Beaufort Sea to support this project

Dr. Chun Yang: Emergencies Science and Technology Section, Environment and Climate Change Canada: Contributed extensively in developing the analytical method to measure oil extracted from OSAs.

Mike Landriault: Emergencies Science and Technology Section, Environment and Climate Change Canada: Contributed extensively to chemistry works

Alaa Alsaafin: Biochemistry and Biotechnology, Carleton University: Conducted extensive analytical experiments on oil weathering and measurement of their physiochemical properties.

Stephen Pynenburg, Nanotechnology Engineering, University of Waterloo: Conducted extensive measurements of IFT under various conditions

Brian Chan, Nanotechnology Engineering, University of Waterloo: Conducted extensive measurements of IFT and droplet formation under various condition

Erica Lynn Wintjes, Nanotechnology Engineering, University of Waterloo: Conducted extensive experiments on OSA formation

Ngai Yan Lau, Nanotechnology Engineering, University of Waterloo: Conducted extensive experiments on OSA formation

Nathaniel Joseph Zavitz, Nanotechnology Engineering, University of Waterloo: Contributed to the development of the droplet imaging setup and conducted extensive measurements on droplet formation

Ayah Alsaafin: Neuroscience, Carleton University: Conducted extensive experiments on OSA formation

Theodora Li: Chemistry, Carleton University: Conducted extensive experiments on OSA formation

Meaghan Keon: Environmental Engineering, Carleton University: Conducted extensive experiments on formation OSAs and measurement of their physical properties

Nicolas Bialik: Environmental Engineering, Carleton University: Conducted extensive experiments on formation OSAs and measurement of their physical properties

Table of Contents

List of Figures

List of Tables

1. Introduction

1.1. Scope of the problem

Several recent studies have shown that aggregation between suspended oil droplets and suspended particulate matter (SPM), which leads to the formation of oil-SPM aggregates (OSAs) (Figure 1), has strong control on the fate and behaviour of oil spills in coastal water rich in SPM (Khelifa et al., 2005a, 2008; Sun and Zheng, 2009; Gong et al., 2014). The authors are not aware of any study that addressed this process for the Beaufort Sea and Mackenzie River Delta water system.

This study aimed to conduct an extensive laboratory study to establish quantitative understanding of OSA formation using Beaufort Sea crude oils and several natural sediments from the Mackenzie River Delta and Norman Wells, NWT.

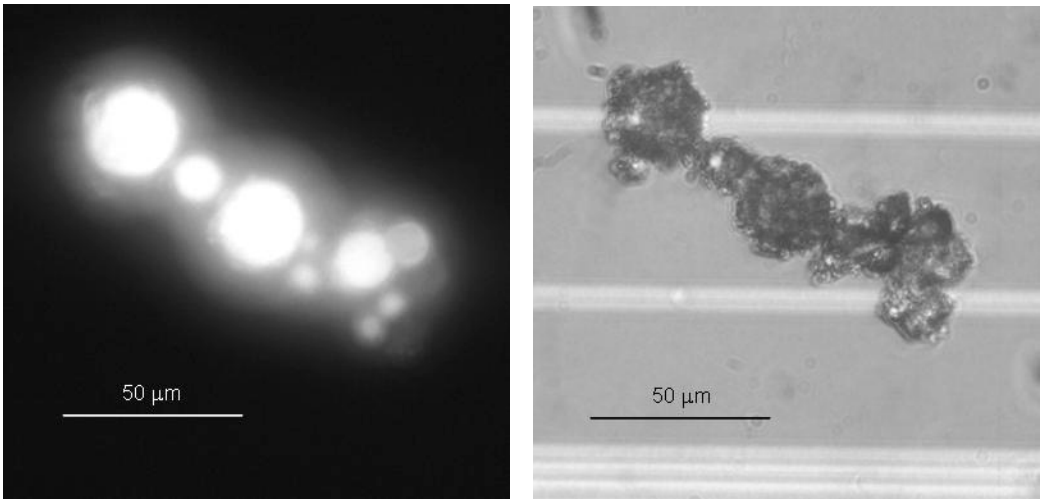

Figure 1. Photomicrographs of OSAs obtained with Heidrun oil and chalk using epi-fluorescence (left) and transmitted light (right). Oil droplets are transparent particles (left) surrounded by dark sediment flocs (right). From Khelifa et al. (2005b).

1.2. Goals and objectives

The goals of this study are to establish quantitative knowledge regarding:

1) the potential of physically dispersed Beaufort Sea crudes oils to aggregate with suspended sediments present in the Mackenzie River Delta

2) the potential of physically dispersed Norman Wells crudes oil to aggregate with suspended sediments present in the Mackenzie River in Norman Wells.

2) the potential of chemically dispersed Beaufort Sea crudes oils to aggregate with suspended sediments present in the Mackenzie River Delta

3) physical properties of OSAs formed with Beaufort Sea and Norman Wells crude oils

4) the potential of sedimentation of the crudes mentioned above in these two water systems due to oil-suspended sediment aggregation.

To achieve these goals, the study has the following objectives.

1) To conduct this study using crude oils obtained from previous oil explorations in the Beaufort Sea and Norman Wells. Crude oils available at ESTS for in this project are: Amauligak, Atkinson, and Issungnak from the Beaufort Sea; and Norman Wells located on the Mackenzie River, NWT..

2) To measure key physical properties of the oil samples mentioned above.

3) To use Corexit EC9500A for dispersant to chemically disperse these oils.

4) To establish quantitative understanding on the effects of chemical dispersant on the reduction of the oil-seawater interfacial tension and the resulting effects on oil dispersion at the freezing temperature. The spinning drop and pendant technologies available at ESTS will be used to achieve this objective. The focus will be on the evaluation of the effects of dispersant-to-oil ratio (DOR) on these processes.

5) To conduct extensive bench-scale testing of oil-sediment interaction using Beaufort and Norman Wells oils discussed above and sediment samples from the Norman Wells and Mackenzie River Delta and at low temperatures with and without chemical dispersant.

6) To compile the new knowledge and make it available to the oil spill community to support both the response and research on spills from Norman Wells and Beaufort Sea crude oils.

2. Oil samples

Four crude oil samples were used to conduct this R&D project. Three were from the Beaufort Sea, Amauligak, Atkinson and Issungnak, and one from Norman Wells located on the Mackenzie River in NWT. These oils were collected from exploratory drilling in the Canadian Arctic in the 1980s. ESTS obtained samples of these oils decades ago. They were stored in sealed drums and do not appear to have significantly weathered based on comparison of physical properties with those measured at the time the samples were acquired.

2.1. Oil physical properties

Eight key physical properties of the oil samples were measured for four stages of weathering of about 0, 10, 20, and 30 % evaporative mass loss at atmospheric pressure. These properties are density, viscosity, surface tension, oil/freshwater interfacial tension, oil/seawater interfacial tension, water content, asphaltenes content, and wax content. The following sections provide detailed descriptions of the analytical procedures used to measures these properties. Results are summarized in Table 1.

2.1.1. Artificially weathered oil samples

Weathered oil samples were produced using a Buchi Rotovapor model R220 with integral water bath (20-L capacity) and a 10-L spherical flask. Two litres of sample were weathered at a time with the bath set to 80 ºC and a rotation rate of 135 RPM. The evaporator was set with an open venting port to maintain atmospheric pressure. A Millipore vacuum pump provided air flow of 13 litres per minute. A sub-sample of the oil is weathered for 48 hours to obtain a highly weathered sample that is quantified for the mass loss. An additional 2 sub-samples were then weathered to yield mass loss values of 1/3 and 2/3 the mass loss of the highly weathered sample.

2.1.2. Oil properties analysis

Density – The density of the oil, in g/mL, is measured using an Anton Parr DMA 48 digital density meter following ASTM Method D5002 (ASTM, 2009), controlled at the temperature of interest to ±0.01 ºC.

Viscosity – The dynamic viscosity was measured using a Thermo-Haake VT550 viscometer with concentric cylinder geometries: NV for viscosities <70 mPa.s, and SV1 for viscosities above 70

mPa.s, at shear rates of 1000 s-1 and 100 s-1 respectively. Temperature of measurement was as noted, controlled to ±0.1 ºC

Interfacial Tension – The interfacial tension of the oil with fresh water, 3.3% sodium chloride brine, and air were determined using an optical CAM200 pendant drop apparatus from KSV Instruments with associated software. A J-hook syringe needle was used for inverting the drop in water. The temperature was controlled to ±0.5 ºC

Asphaltene Content - The asphaltene content of an oil sample was determined by precipitation in excess n-pentane and filtering on a 0.45 µm filter to obtain a mass ratio.

Wax Content – The wax content of an oil was determined on the de-asphaltenized maltene fraction by precipitation from a 1:1 mixture of methyl ethyl ketone and dichloromethane at -30 ºC and filtering on a 0.45 µm filter.

Table 1. Measured physical properties of the oil samples used in this study

Oil Type	Weathering (evaporation loss) (%)	Density (g/mL)		Viscosity (mPa·s)		Surface Tension (mN/m)		Interfacial Tension (mN/m)				Water Content (%w/w)	Asphaltenes (%w/w)	Wax Content (%w/w)
								Water		Seawater				
		0 ºC	15 ºC	0 ºC	15 ºC	0 ºC	15 ºC	0 ºC	15 ºC	0 ºC	15 ºC			
Amauligak	0.00	0.8938	0.8833	21.30	12.34	29.79	28.33	23.19	23.09	22.73	22.29	0.04	0.12	0.83
	9.60	0.9070	0.8968	41.55	21.62	31.27	28.75	23.88	23.08	23.47	22.83	0.02	0.15	1.07
	19.03	0.9154	0.9054	84.15	36.85	31.68	29.94	23.97	23.34	23.75	22.56	0.02	0.18	1.15
	28.38	0.9221	0.9122	166.1	63.42	32.14	30.48	21.89	21.44	21.87	20.64	0.01	0.31	1.26
Atkinson	0.00	0.9204	0.9103	130.9	57.96	30.62	27.08	30.51	30.50	30.52	29.55	0.05	1.47	1.15
	8.70	0.9360	0.9260	412.43	140.27	31.70	28.75	32.43	32.73	32.17	31.67	0.36	1.94	1.01
	17.80	0.9541	0.9437	2,582	673	32.89	31.41	24.69	26.64	27.62	26.28	0.00	2.79	1.06
	26.19	0.9643	0.9534	9,601	1,867	34.37	31.81	22.23	22.12	20.55	20.89	0.02	3.59	1.02
Issungnak	0.00	0.8701	0.8573	37.24	7.32	29.50	27.95	NM	18.21	NM	16.21	0.01	0.17	3.08
	9.75	0.8814	0.8678	381.97	13.02	NM	28.56	NM	18.89	NM	16.17	0.01	0.21	3.07
	19.35	0.8905	0.8766	414.07	19.92	NM	30.12	NM	18.70	NM	16.67	0.01	0.18	2.38
	32.42	0.9015	0.8873	7864	96.00	NM	31.85	NM	16.16	NM	16.16	0.01	0.28	2.51
Norman Wells [1983]	0.00	0.8489	0.8375	11.54	7.46	27.49	25.78	24.44	24.74	24.77	24.84	0.03	0.43	3.46
	14.46	0.8784	0.8672	26.53	15.83	29.04	27.51	25.63	25.64	26.06	26.06	0.02	0.48	4.64
	28.69	0.8999	0.8888	144.3	47.1	30.38	28.16	26.36	25.60	26.34	26.46	0.01	0.64	5.48
	43.07	0.9205	0.9087	1259.5	242.7	32.14	28.68	NM	24.33	NM	24.90	0.01	0.94	7.67

NW: not measurable by the method used due to viscoelastic effects

2.2. Selected oils for OSA Formation Study

Considering the measured physical properties of the oils listed in Table 1, the preliminary testing and the actual state-of-knowledge regarding OSA formation, Issungnak crude oil samples present a weak potential to form OSAs. As such, only OSA formation with Amauligak, Atkinson and Norman Wells crude oils is discussed in this report.

3. Sediment samples

Sediment samples used in this study include one standard reference material SRM 1941B from the National Institute of Standards and Technology (NIST), four samples of bottom/shorelines sediment from the Beaufort Sea and three from Norman Wells, NWT.

Regarding natural sediments, several sampling campaigns of bottom/shoreline sediments have been conducted to support this project. This sampling works were conducted by two key groups of very kind collaborators.

Norman Wells Sediments

Brian Yurris and **Ryan Lennie**
Water Survey of Canada
Environment and Climate Change Canada
P.O. Box 2310
5019 52nd Street 4th Floor
Yellowknife, NT X1A 2P7
Phone (867) 669-4778
Fax (867) 669-4750

Beaufort Sea Sediments

Dustin Whalen
Geological Survey of Canada
Bedford Institute of Ocean.
Natural Resources Canada
Dartmouth, NS B2Y 4A2
Phone: 902-426-0652
Fax: 902-426-4104

3.1. Sediment sampling from Norman Wells

Sampling of bottom/shoreline sediments from Norman Wells was conducted by Brian Yurris and Ryan Lennie from the Water Survey of Canada of Environment and Climate Change Canada. With their very kind collaboration, 12 sites of the Mackenzie River were sampled at Norman Wells. The locations of the sampling sites are shown in Figure 2. Their coordinates are shown in Table 2. An overview of the sampling area is shown in Figure 3. All sediments were sampled wet and were stored wet at 4 ^{o}C.

Figure 2. Geographical locations of the 12 sediment sampling sites in Norman Wells.

Figure 3. Overview of the sediment sampling area in Norman Wells. (Photo from Brian Yurris)

Table 2. Sampling date and coordinates of the sediment sampling sites in Norman Wells

Sampling Site	Sampling Date	Latitude (°)	Longitude (°)
1	10/10/2013	65.27877	126.84326
2	10/10/2013	65.27143	126.78201
3	26/09/2013	65.26290	126.84821
4	26/09/2013	65.25013	126.93597
5	26/09/2013	65.23582	126.88205
6	26/09/2013	65.22766	126.77388
7	26/09/2013	65.24944	126.75050
8	26/09/2013	65.29072	126.99646
9	26/09/2013	65.27663	126.99045
10	26/09/2013	65.27361	127.04170
11	26/09/2013	65.28188	126.88452
12	26/09/2013	65.27030	126.88730

3.2. Sediment sampling from the Beaufort Sea

Sampling of bottom/shoreline sediments from the Mackenzie River Delta in the Beaufort Sea was conducted by Dustin Whalen and his team from the Geological Survey of Canada of natural Resources Canada. With their very kind collaboration, 8 sites of the Mackenzie River Delta were sampled. The locations of the sampling sites are shown in Figure 4. Their coordinates are shown in Table 3. The sampling team are shown in Figure 5. All sediments were sampled wet and were stored wet at 4 ^{o}C.

Table 3. Sampling date and coordinates of the sediment sampling sites in the Mackenzie River Delta in the Beaufort Sea

Sampling Site	Sampling Date	Latitude (^{o})	Longitude (^{o})
BS-Site 1	14/08/2013	69.40550	133.16320
BS-Site 2	15/08/2013	68.91536	136.63432
BS-Site 3	04/08/2013	69.44116	133.73802
BS-Site 4	09/08/2013	69.47328	134.92150
BS-Site 5	11/08/2013	70.27201	135.71198
BS-Site 6	11/08/2013	70.00090	137.00371
BS-Site 7	10/08/2013	69.29082	135.85470
BS-Site 8	10/08/2013	69.43580	135.83921

Figure 3. Geographical locations of the 8 sediment sampling sites in the Mackenzie River Delta in the Beaufort Sea.

Figure 5. The sampling team for the Mackenzie Rivera Delta sediment. Dustin Whalen shown at the front of the picture. (Photo from Dustin Whalen)

3.3. Selected sediment samples for the OSA formation experiments

Three sediment samples from Norman Wells and four from the Mackenzie River Delta were selected to conduct the OSAS formation study in this project. These samples were selected based on their fine contents. It is well established that sediment rich in fines (less than about 10 μm in size) are good sediments to form OSA (Khelifa et al. 2008a). Pictures of the sampling sites NW-Site 2 in Norman Wells and BS-Site 2 in the Mackenzie River Delta are shown in Figures 6 and 7, respectively.

Figure 6. Brian Yurris from Water Survey of Canada sampling sediment from NW-Site 2 in Norman Wells (Photo from Brian Yurris)

Figure 7. Overview of the sampling area in sampling site BS-Site 2 in the Mackenzie Rivera Delta sediment. (Photo from Dustin Whalen)

3.4. Organic matter content of the selected sediment samples

After fine content, organic matter content in natural sediments is known to play a second major role in promoting the formation of OSAs (Khelifa et al. 2008). Organic matter content (OMC) in the selected sediment samples was measured using the Loss-on-Ignition (LOI) method. The procedure used to conduct this measurement was based on the recommendations presented recently by Hoogsteen et al (2015). For each sediment type, three samples (triplicate) of about 3 g each were first dried at 60 ^{o}C in the oven for 36 hours. After first weighing, they were burned at 550 ^{o}C in a furnace for three hours and then weighed for the second time. The difference of weight represents the mass of OMC. A picture of the crucibles containing sediment samples introduced into the furnace is shown in Figure 8. Results are shown in Table 4

Figure 8. A picture of the crucibles containing sediment samples when introduced into the furnace during the Loss-on-Ignition experiment to measure organic matter content in the sediments.

Table 4. Organic matter content in the selected sediment samples measured using the Loss-on-Ignition method

Sampling Site	Organic Content w/w (%)	Standard deviation (w/w (%)
BS-Site 1	5.23	0.13
BS-Site 2	4.69	0.33
BS-Site 3	3.24	0.03
BS-Site 4	3.49	0.21
NW-Site 1	4.03	0.08
NW-Site 2	4.05	0.06
NW-Site 3	3.20	0.02

3.5. Size distribution of the selected sediment samples

Gain size distributions of each sediment samples was measured 10 times using the Malvern Mastersizer 2000 particle size analyser (Figure 9)following standard procedure provided by Malvern Instruments Ltd. Average size distributions of the four sediment samples used in OSA experiments and settling process are shown in Figure 10.

Fine contents for these sediment samples are shown in Table 5 for different size ranges

Figure 9. A picture of the ESTS's Malvern Mastersizer 2000 particle size analyser with the Hydro 2000 Unit used to measure grain size distribution of the selected sediment samples.

Table 5. Fine content contain in the selected sediment samples

Sediment	Fine content (vol %)			
	D<=2.2 um	D<=5 um	D<=10 um	D<=60 um
SRM-1941b	6.3	30.3	52.9	91.3
BS-Site 1	3.7	24.5	42.4	87.8
BS-Site 2	1.3	7.7	14.6	86.5
BS-Site 3	2.2	10.7	22.0	82.0
BS-Site 4	0.9	6.8	15.4	89.8
NW-Site 1	1.5	8.2	17.4	80.5
NW-Site 2	1.7	9.5	20.8	87.6
NW-Site 3	2.0	10.6	22.4	88.7

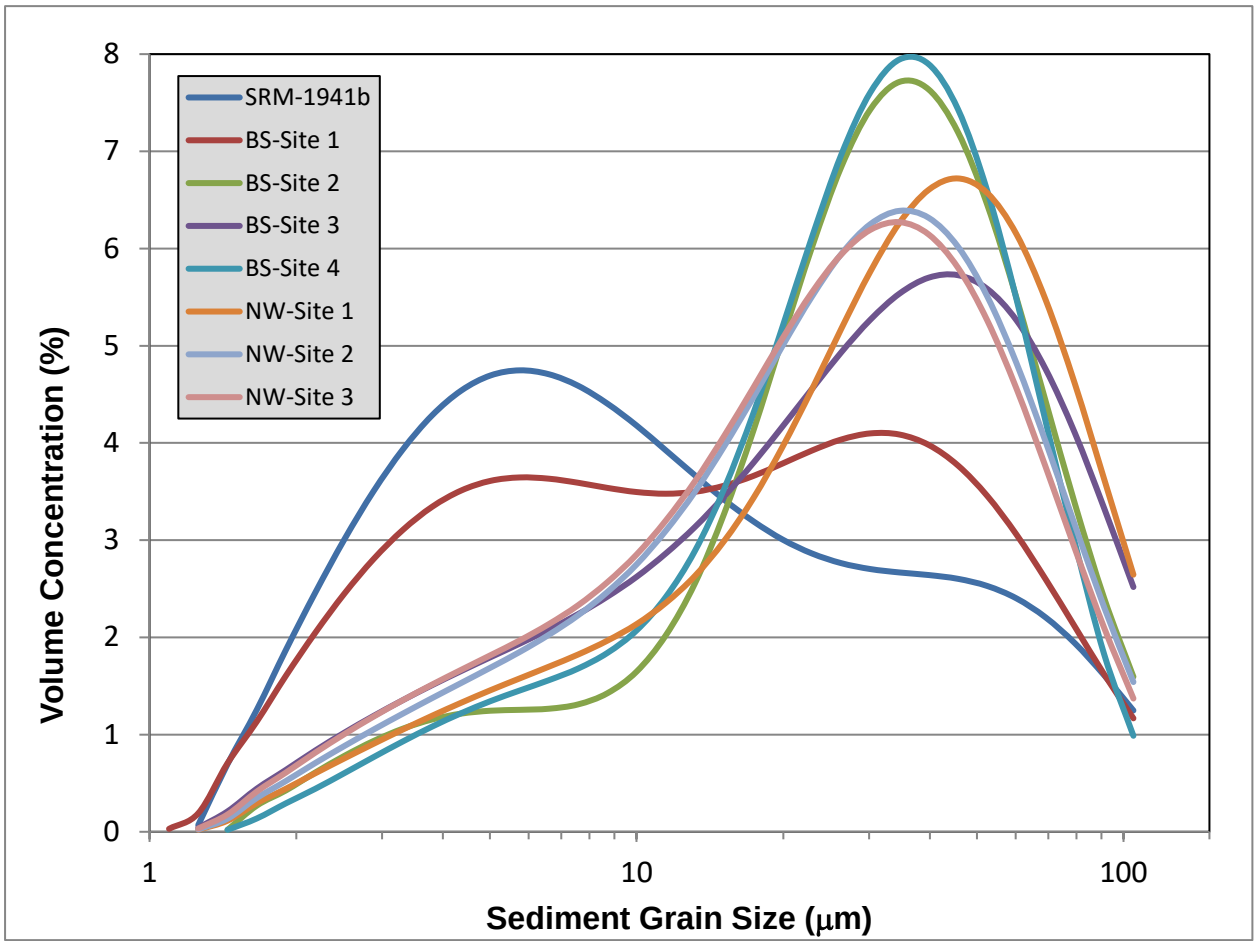

Figure 10. Measured grain size distributions of the selected sediment samples for OSA experiments.

4. Oil dispersion

Oil dispersion was studied in the project to establish a quantitative understanding of the process of droplet formation. This includes two following major related topics:

1. in-depth understanding of the variations of the oil/brine interfacial tension (IFT) with the environmental conditions and the dispersant-to-oil ratio (DOR).
2. in-depth understanding of the variations of oil droplet size distribution with the environmental conditions and the dispersant-to-oil ratio (DOR).

4.1. IFT measurement

Oil/brine interfacial tension (IFT) was measured using two different state-of-the-art instruments. For relatively high IFT, Pendant Drop instrument KSV CAM200 was used (Figure 11). Spinning Drop Tensiometer SITE100 manufactured by KRUSS was used to measure small values of IFT, especially when dispersant were used.

Figure 11. Instruments used to measure oil/brine interfacial tension: KSV CAM200 Pendant Drop (left), and KRUSS spinning Drop SITE100 (right).

4.1.1. Effects of oil types and weathering

Air/oil, water/oil and seawater/oil interfacial tensions were measured for all the Arctic oils with different stages of weathering. The measurements were performed at 15 ^{o}C and a freezing temperature of 0 ^{o}C. Results are summarized in Table 6

Table 6. Interfacial tensions measured for different Arctic oils and different weathering conditions

Oil	%Evap loss	Interfacial Tension (mN/m)					
		Air/Oil		Water		Seawater	
		0 ºC	15 ºC	0 ºC	15 ºC	0 ºC	15 ºC
Amauligak	0.00	29.79	28.33	23.19	23.09	22.73	22.29
	0.10	31.27	28.75	23.88	23.08	23.47	22.83
	0.19	31.68	29.94	23.97	23.34	23.75	22.56
	0.28	32.14	30.48	21.89	21.44	21.87	20.64
Atkinson	0.00	30.62	27.08	30.51	30.50	30.52	29.55
	0.09	31.70	28.75	32.43	32.73	32.17	31.67
	0.18	32.89	31.41	24.69	26.64	27.62	26.28
	0.26	34.37	31.81	22.23	22.12	20.55	20.89
Norman Wells	0.00	27.49	25.78	24.44	24.74	24.77	24.84
	0.14	29.04	27.51	25.63	25.64	26.06	26.06
	0.29	30.38	28.16	26.36	25.60	26.34	26.46
	0.43	32.14	28.68	NM	24.33	NM	24.90

Note: 0°C Oil-Water measurements were done at 32.5-33°F (~0.3-0.6°C)
NM - Not Measurable using Pendant Drop - No droplet formed/incorrect droplet shape

4.1.2. Effects of water temperature

In addition to the data shown in Table 6, the effects of temperature on IFT were studied for the Amauligak crude oil and at 5 ppt water salinity. Results are shown in Figure 12.

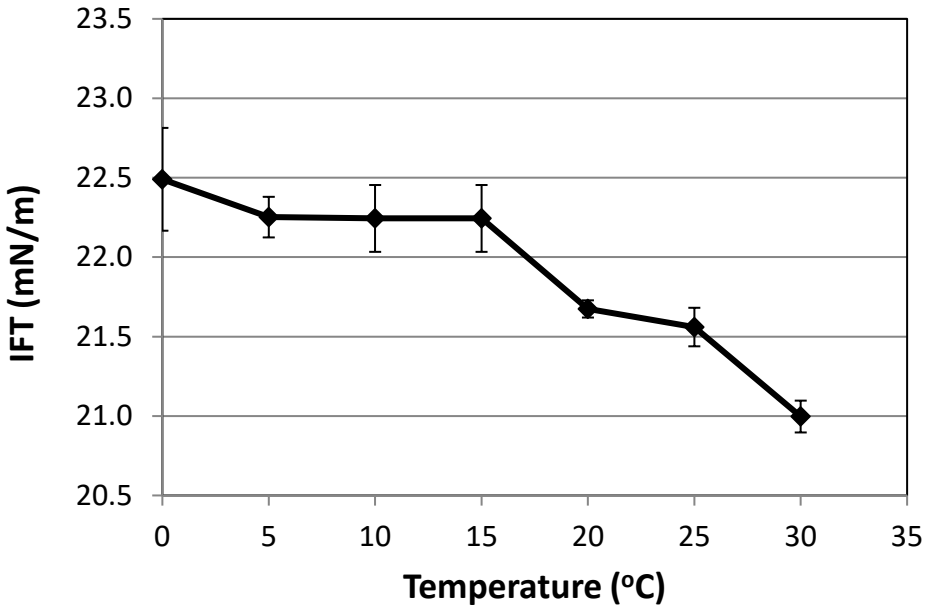

Figure 12. Oil/brine interfacial tension measured at different temperatures with Amauligak crude oil, 5 ppt water salinity and no dispersant.

4.1.3. Effects of water salinity

The effects of water salinity on IFT were studied for the Amauligak crude oil and at 15 °C. Results are shown in Figure 13. The vertical scale was kept the same as in Figure 12 to facilitate visual comparison between the effects water temperature and water salinity on IFT.

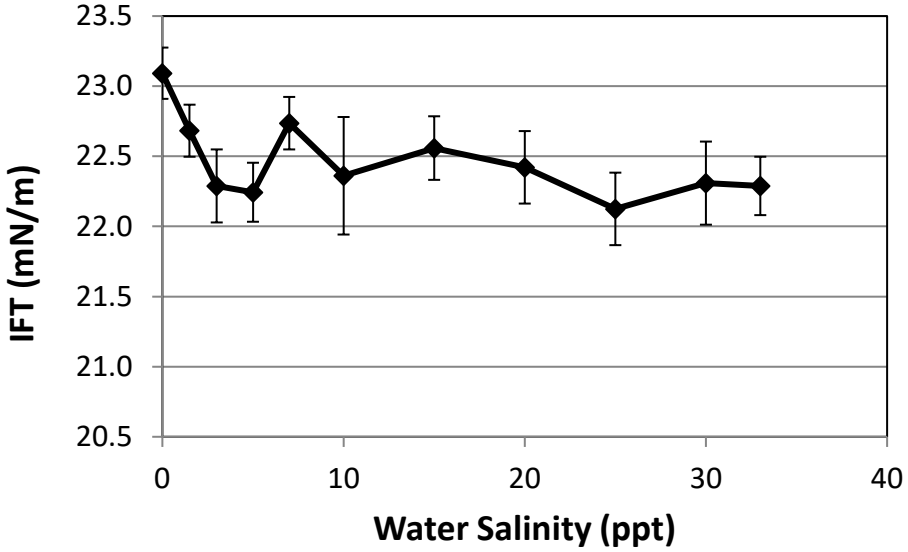

Figure 13. Oil/brine interfacial tension measured at different water salinities with Amauligak crude oil, 15 °C and no dispersant.

4.1.4. Effects of dispersant (DOR)

The effects of dispersant dosage (DOR) on IFT were studied for the Amauligak crude oil and at 15 ^{o}C and water salinity of 5 and 33 ppt. Results are shown in Figures 14 and 15.

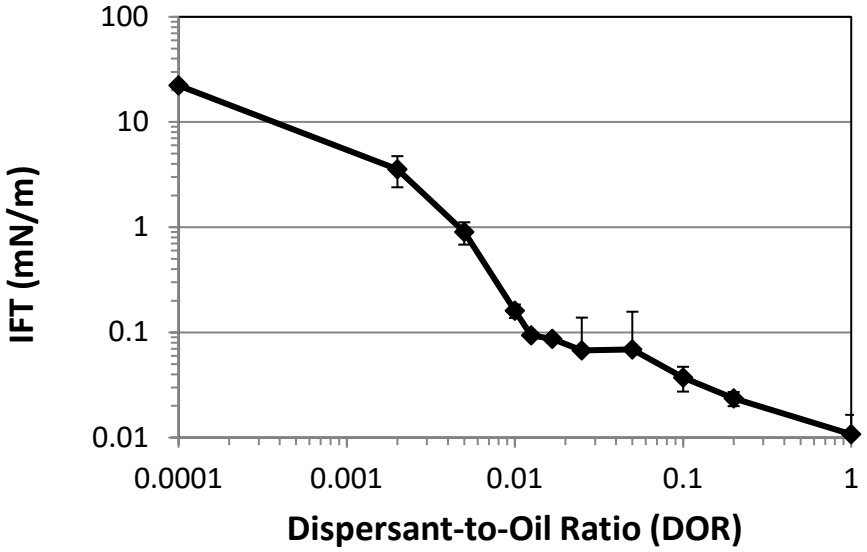

Figure 14. Oil/brine interfacial tension measured at different DOR with Amauligak crude oil, 15 ^{o}C and 5 ppt water salinity

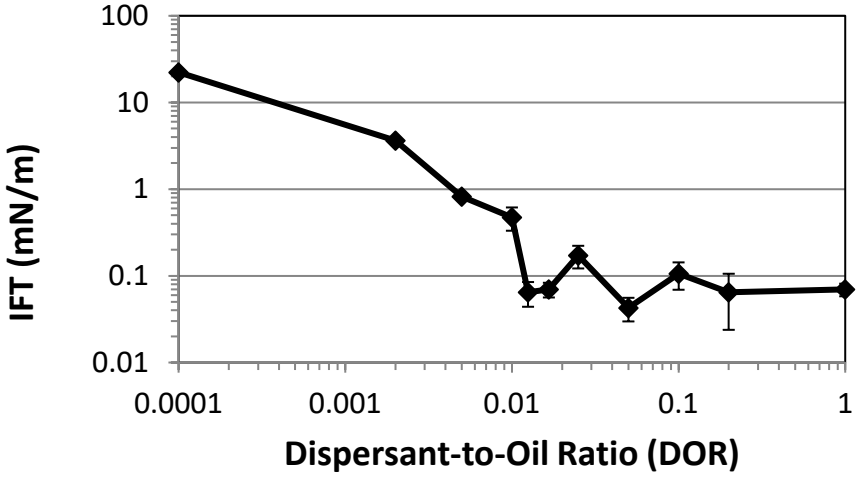

Figure 15. Oil/brine interfacial tension measured at different DOR with Amauligak crude oil, 15 ^{o}C and 33 ppt water salinity

4.2. Droplet formation

The second component of oil dispersion is to study droplet formation under various conditions. This was done using an in-house setup shown in Figure 16. This included an orbital shaker, a high resolution DSLR camera equipped with proper lens and extension tube and a back light to illuminate oil droplets dispersed in a 125 mL Erlenmeyer flask.

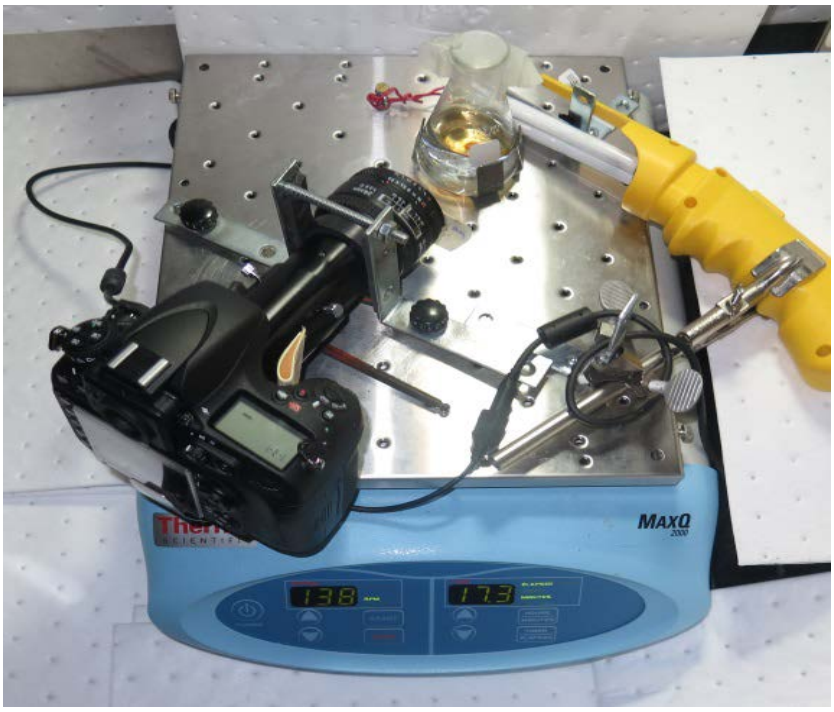

Figure 16. In-house developed setup used to study droplet formation.

Examples of pictures obtained with this setup are shown in Figures 17.

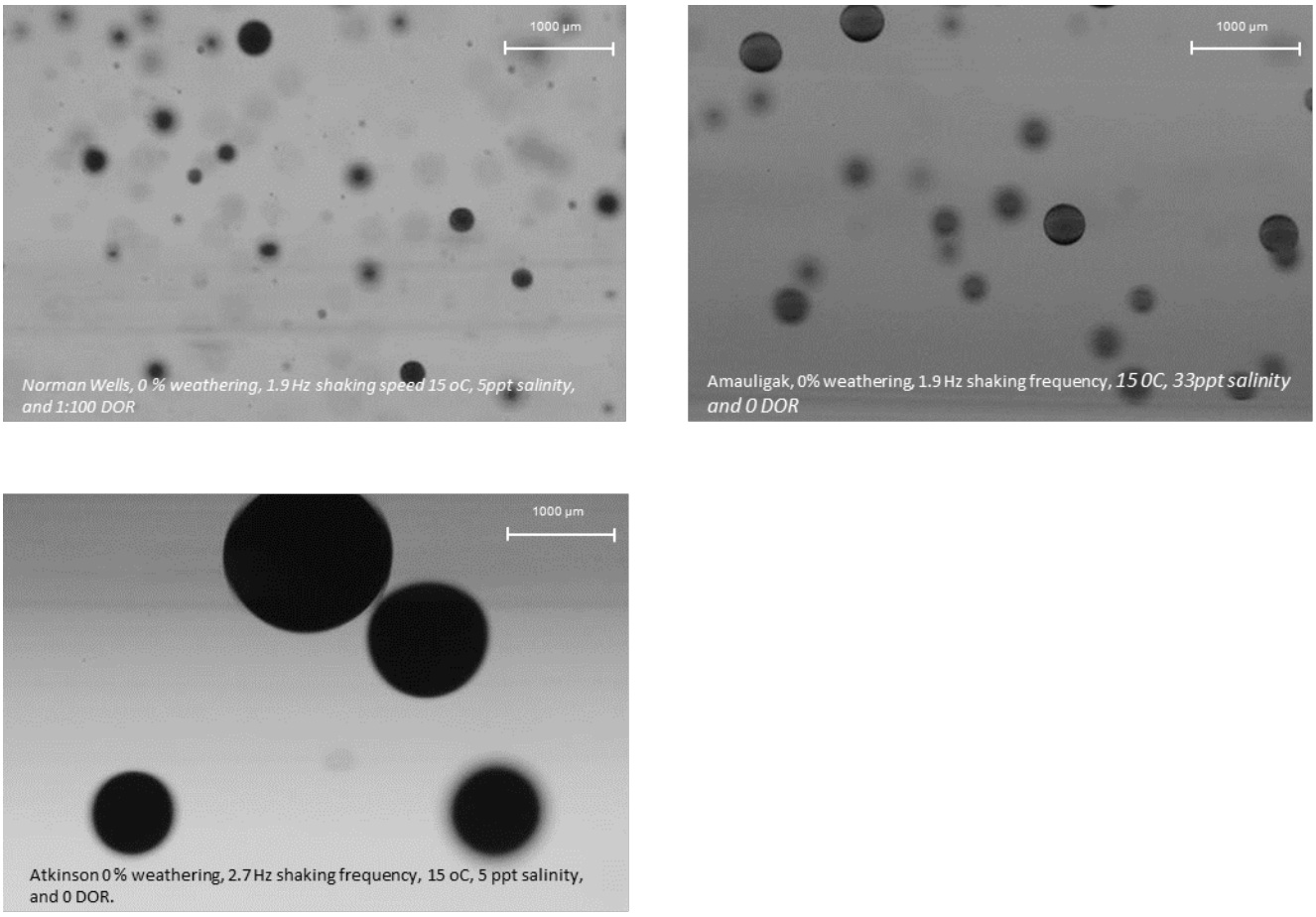

Figure 17. Examples of pictures of dispersed oil droplets obtained under different conditions, as shown on each picture.

To measure the size distribution of oil droplets, thousands of images had to be analyzed using a computer program developed in-house using Matlab software. Size distributions measured at 15 ^{o}C and using 33ppt water salinity, 2.3 Hz mixing speed, and the three crude oils are shown in Figures 18-21. In all these figures, the “Oil Droplet Size” (horizontal axis) refers to the diameter of the droplets measured using image analysis. At zero DOR (i.e. with no dispersant), the dispersion of the three oils was not significant.

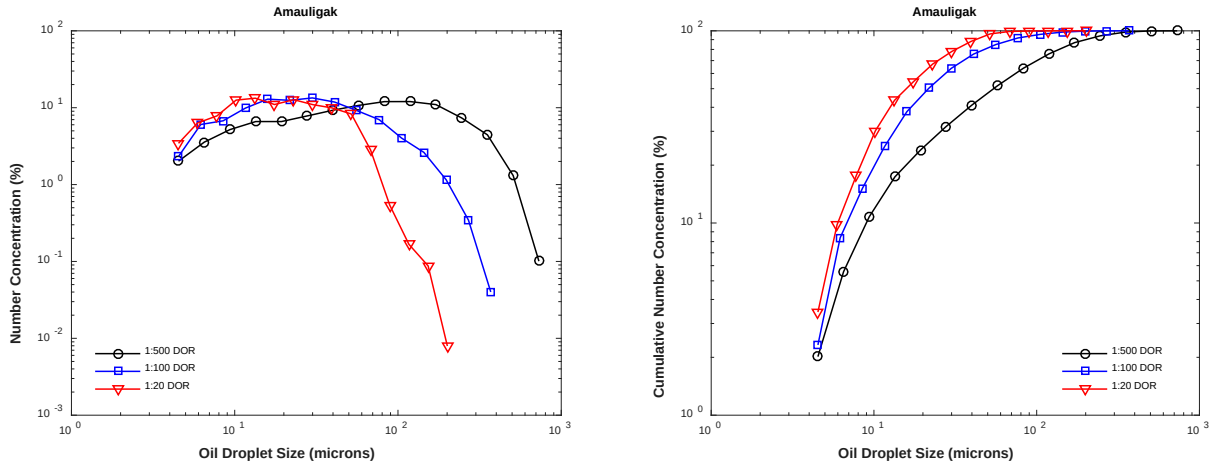

Figure 18. Number (left) and cumulative (right) size distributions measured with Amauligak crude oil at 15 ^{o}C using water salinity of 33 ppt and mixing speed of 2.3 Hz.

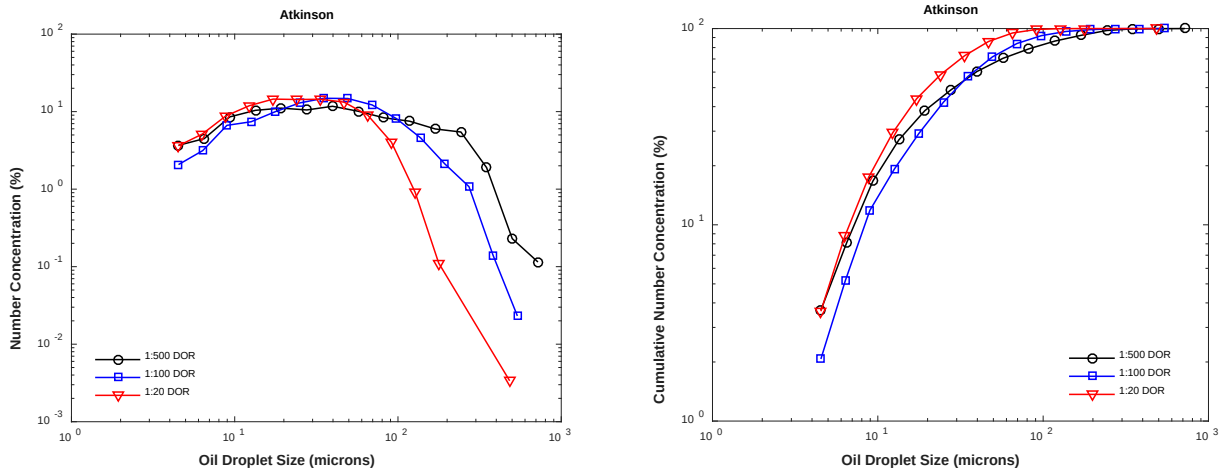

Figure 19. Number (left) and cumulative (right) size distributions measured with Atkinson crude oil at 15 ^{o}C using water salinity of 33 ppt and mixing speed of 2.3 Hz.

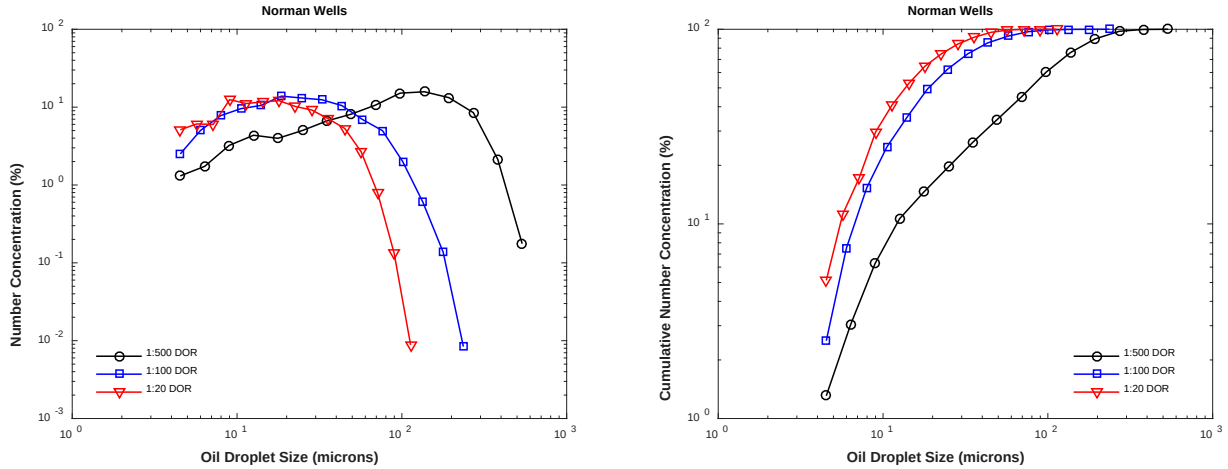

Figure 20. Number (left) and cumulative (right) size distributions measured with Norman Wells crude oil at 15 ^{o}C using water salinity of 33 ppt and mixing speed of 2.3 Hz.

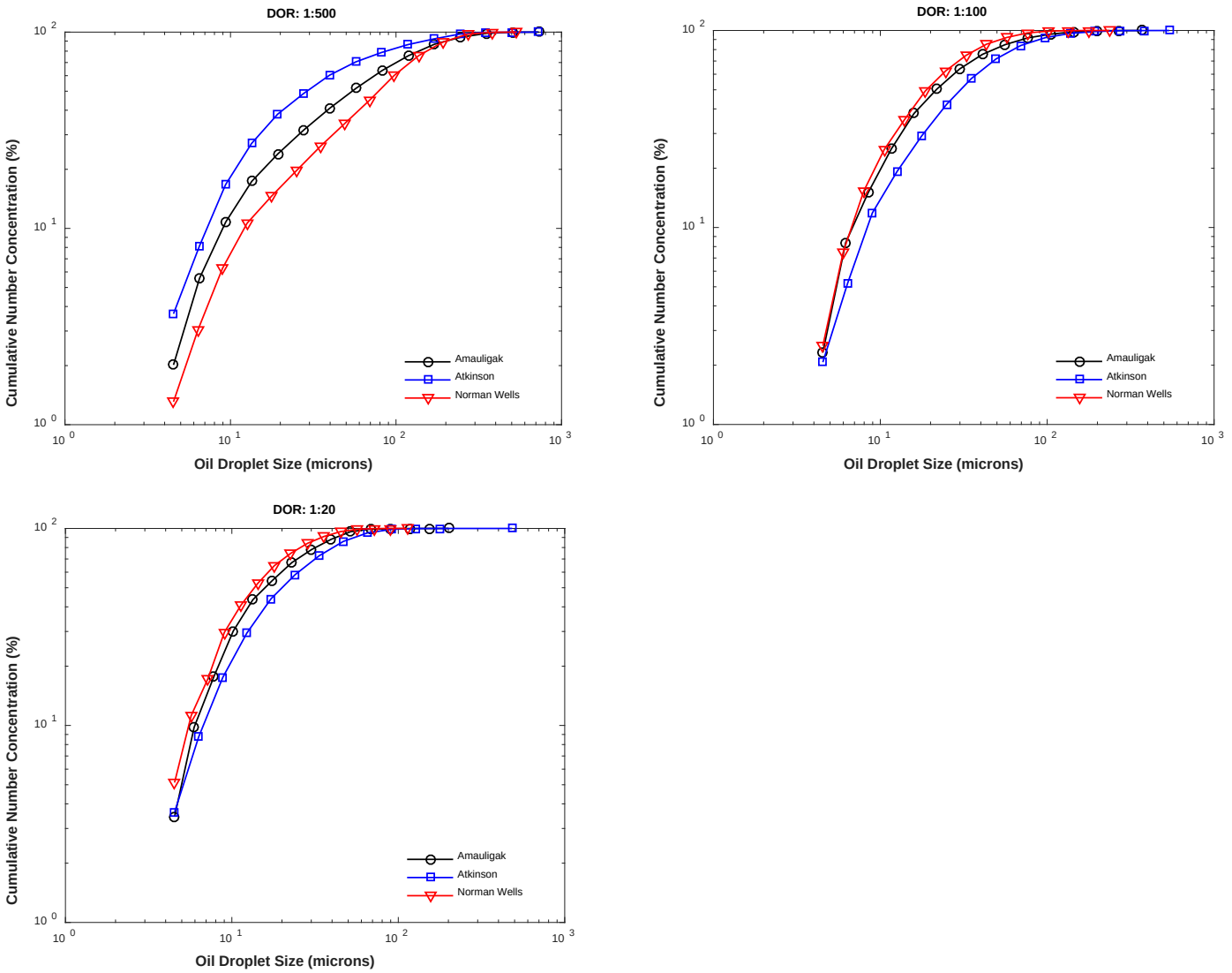

Figure 21. Comparison between measured size distributions of oil droplets obtained with the three Arctic oils at 15 ^{o}C using water salinity of 33 ppt, mixing speed of 2.3 Hz, and various DOR values.

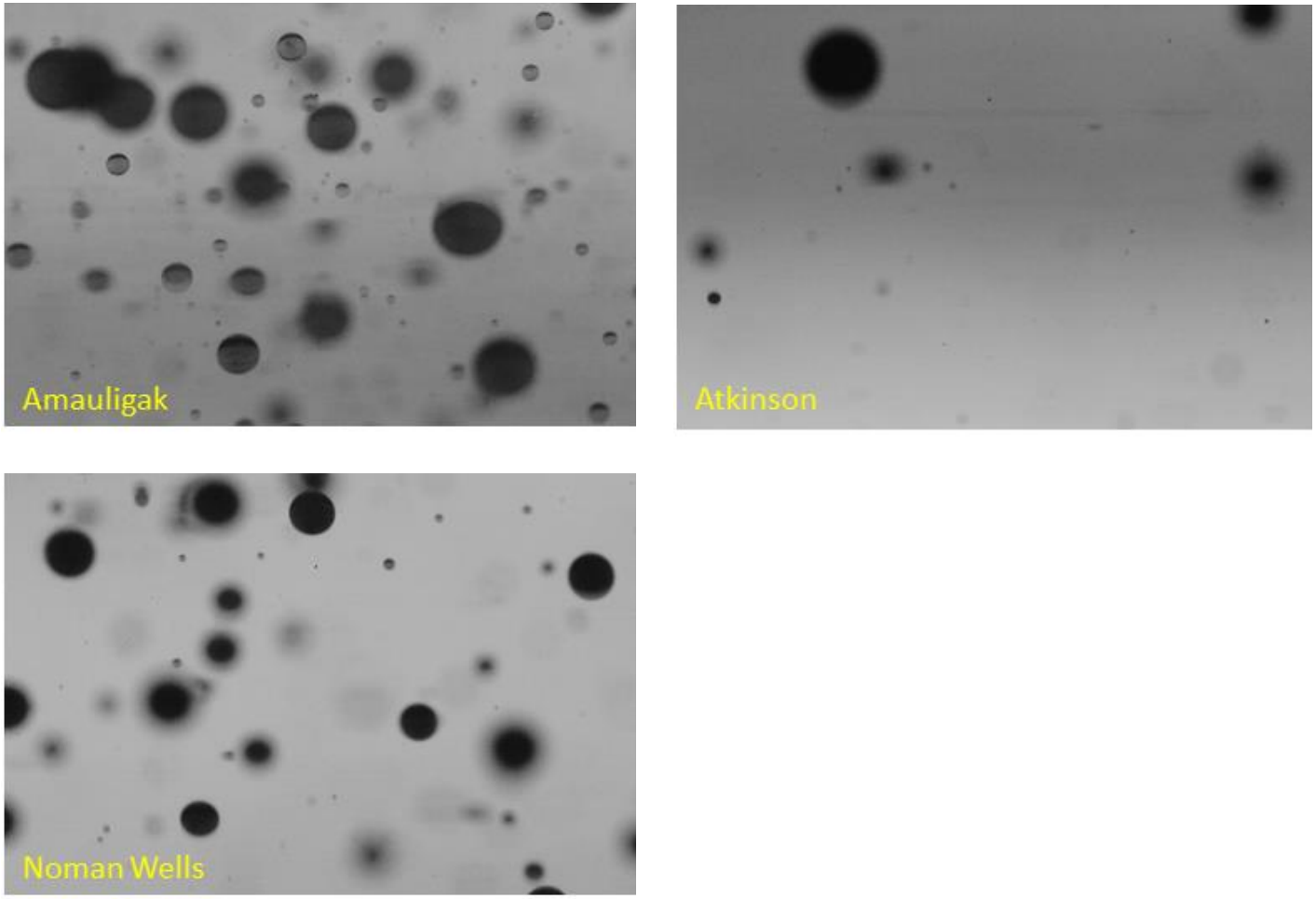

Figure 22. Typical images of oil droplets obtained with the three Arctic oils at 15 ºC using water salinity of 33 ppt, mixing speed of 2.3 Hz, and 1:500 DOR. The scale is the same as in Figure 16.

5. OSA formation

5.1. Procedure

The procedure used to study OSA formation includes several steps. Its development took into consideration the performances and weaknesses of previous methods used to study OSA formation in the laboratory. As the study focuses on oil sedimentation, only negatively buoyant OSAs were measured in this project. The steps of the experimental protocol include OSA preparation, isolation of negatively buoyant OSAs, oil extraction from OSAs, sediment filtration from OSAs, measurement of size and settling velocity of OSAs, calculation of the density of OSAs and microscopic investigation of OSAs using UV epi-fluorescence technique. Detailed description of the procedure is presented Khelifa et al. (2008). However, the quantitation of oil in negatively buoyant OSAs was modified to a gravimetric method.

Briefly, OSAs were prepared using a reciprocating shaker at a constant shaking speed rate of 126 cycles per minute and a constant stroke of 38 mm in a temperature-controlled room using two temperatures of 0 and 15 ^{o}C. Erlenmeyer flasks (500 mL with silicone stoppers) containing 250 mL of water with given salinity were used as reaction chambers (Figure 23). As shown by Weise et al. (1999), Erlenmeyer flasks shaken with a reciprocating shaker simulate a better disruption of the liquid/air interface, as in breaking wave flow, compared to other mixing devices. The sediment phase was added to the water dry for the SRM-1941b sediment and as a suspension for the natural sediments. When the sediment was added dry to water, the flasks were left overnight for sediment hydration. Before adding oil, the flasks were shaken for 5 minutes. A pre-calculated volume of the test oil to deliver 50 mg of oil is added at the water surface using a syringe. For each test oils, the syringe was pre-calibrated to dispense 50 mg of oil. The flasks were then shaken (Figure 23) for a period of three hours and then left to settle overnight in the cold room.

Figure 23. Reaction vessels set for shaking on the reciprocating shaker

The procedure used to separate the negatively buoyant OSAs (Figure 24) was as described in Khelifa et al. (2008). The oil-sediment mixture, which contains sinking OSAs and transferred as a suspension into the separatory funnels, was extracted using distilled-in-glass grade DCM and liquid/liquid extraction procedure. For each sample, the extraction was repeated three times. The DCM to water (suspension) ratio was 1:2 in the first extraction and 1:5 in the subsequent extractions. Preliminary tests showed that no measurable oil amount remained in the sample when a fourth extraction is applied. For each extraction, the water/oil/sediment/DCM mixture was shaken periodically seven times. The extract was passed through a 0.45 µm cellulosic filter under vacuum prior to drying with sodium sulphate. The cellulose filter was preferred as it allows passage of both DCM and water once dried properly.

The extract was then evaporated to about 5 mL using rotary evaporation in boiling flask. The samples were blown down further under nitrogen atmosphere until the DCM is completely dried.

Special care was taken to not over dry the samples. The oil mass was then measured gravimetrically.

Figure 24. Remaining oil-sediment mixture (negatively buoyant OSAs) after carful elimination of the floating materials and water. Samples shown are ready for transfer into separatory funnels. Note the sediment concentration used in this experiment increases from right to left.

5.2. OSA observation using UV epi-fluorescence microscopy

Verification of OSA formation was performed using UV epi-fluorescence microscopy (Khelifa et al., 2018). The setup for UV-fluorescence microscopy (Figure 25) includes Zeiss microscope offering the possibility to observe particles up to 100 times their real size under both transmitted and UV lights and a high resolution digital camera Zeiss AxioCam HRM controlled by a computer. With this setup, particles of 0.1 μm and larger can be measured.

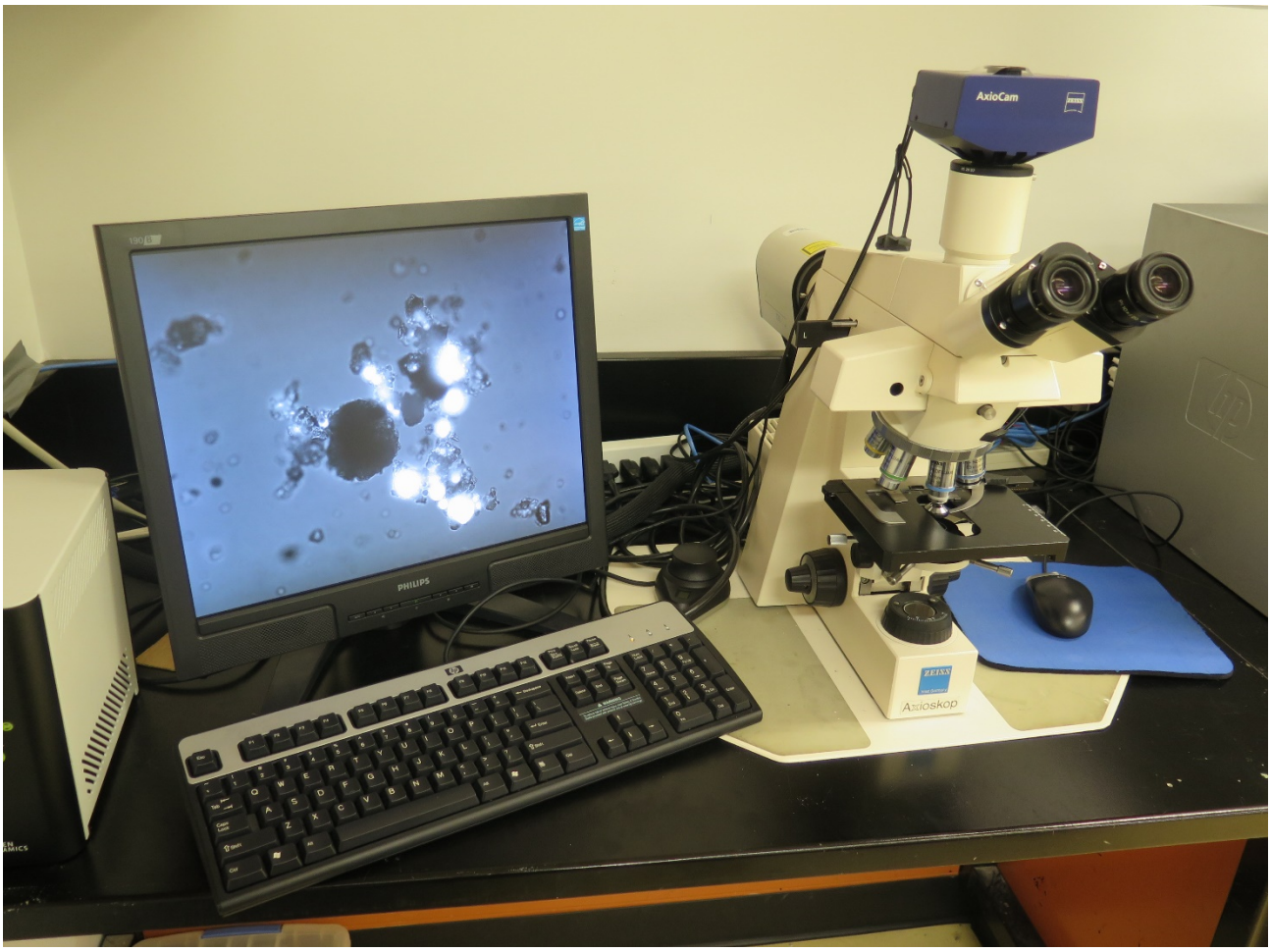

Figure 25. Setup for UV epi-fluorescence microscopy to picture OSAs of 0.1 μm in size and larger. A picture of OSA is displayed on the screen in this picture.

Examples of OSA pictures taken with this step are shown in Figure 26. Clearly, this shows that OSAa do form readily with the three oils with a relatively small concentration of SRM-1941b sediment and a small dosage of Corexit EC9500A as little as 1:500 DOR was applied.

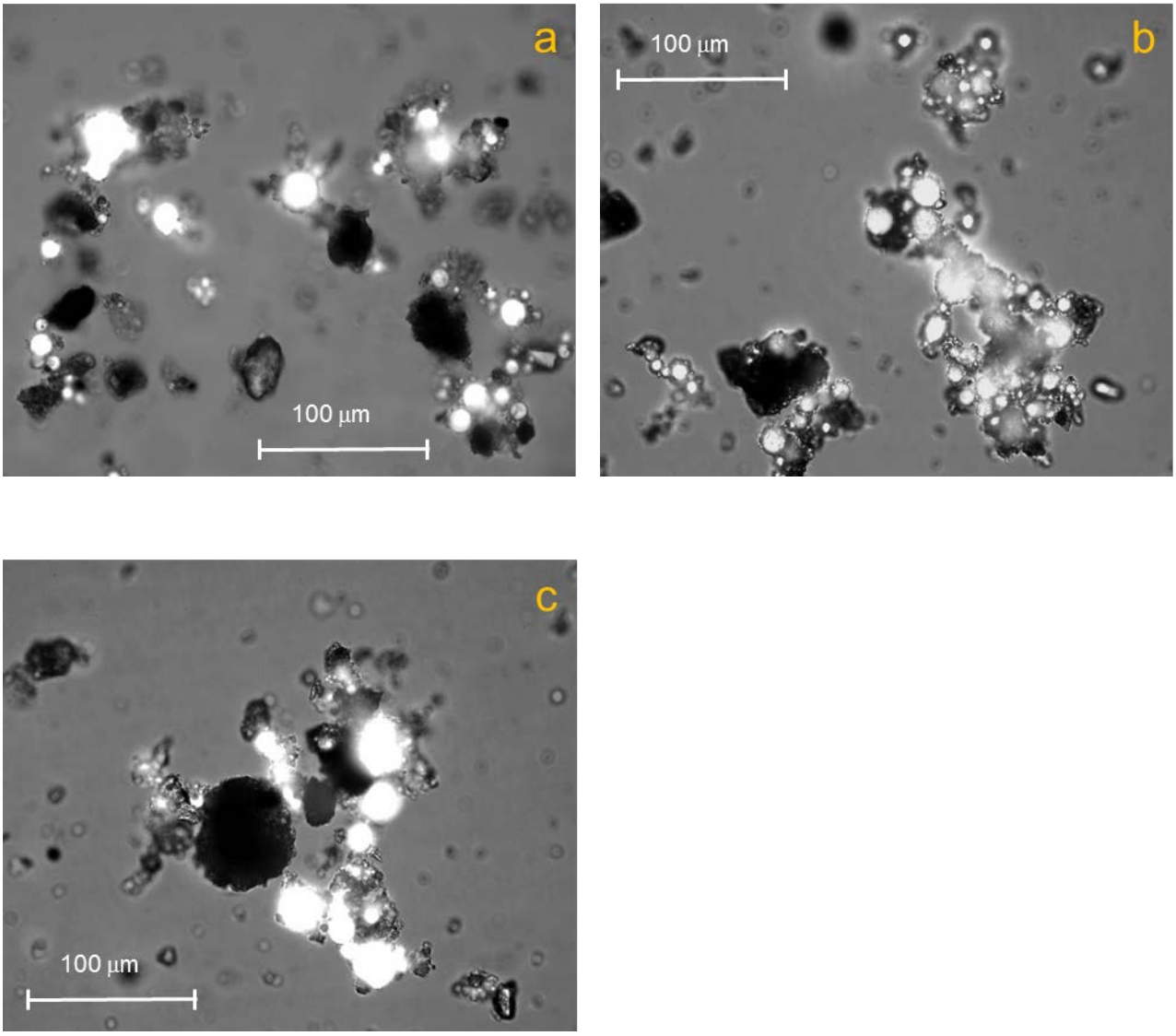

Figure 26. Photomicrographs of negatively buoyant OSAs obtained with: (a) Amauligak crude oil with 1:100 DOR, (b) Atkinson crude oil with 1:60 DOR, and (c) Norman Wells crude oil with 1:500 DOR at 15 oC, 33 ppt water salinity and with concentration of SRM-1941b sediment of 100 mg/L. In these photomicrographs, oil droplets appear bright (when eliminated with UV light) and sediment fines are dark coating oil droplets. Corexit EC9500A was used in these experiments.

5.3. Experimental results

In this project, OSA formation was studied under various conditions. The parameters that were varied are:

- Oil type

- Sediment type
- Sediment concentration
- Water salinity
- Water temperature
- Dispersant-to-oil ratio (DOR), or dispersant dosage.

Because of the large variety of the conditions used, it was difficult to find a way to present the results without cross assessment of the different parameters. The figures presented in this section were intended to illustrate the effects of a single parameter on OSA formation.

5.3.1. Effects of the oil type for different sediment types and concentrations

Effects of sediment type on OSA formation was studied without chemical dispersant using two water salinities of 0 and 33 ppt, as well as with Corexit EC9500A and seawater at 1:20 DOR. In these series, all experiments were run at 15 ^{o}C using Amauligak, Atkinson and Norman Wells crude oils (0% weathering). For SRM-1941b, BS-Site 1, and BS-Site 2 sediment samples, the experiments were run using seven sediment concentrations: 0, 25, 50, 100, 200, 300 and 400 mg/L. For BS-Site 3 and 4, the OSA experiments were run using a single sediment concentration of 200 mg/L and related results are discussed in section 5.3.3. Results obtained with Amauligak and Atkinson crude oils are shown in Figures 27 and 28, respectively. For each oil, the experiments were repeated for water salinities of 0 and 33 ppt and 0 and 1:20 DOR.

For Norman Wells (Figure 29), the water salinity was kept constant to 0 ppt and no dispersant due to the location of the study area, i.e. freshwater environment.

5.3.2. Effects of water salinity for different sediment types and concentrations.

For the Beaufort Sea sediments from sampling sites BS-Site 1 and 2, the effects of water salinity on OSA formation at variable sediment concentration was studied using two water salinities of 0 and 33 ppt, as shown in Figures 27 and 28.

More in-depth study on the effects of water salinity on OSA formation was conducted using SRM-1941b sediment at different sediment concentration (Figure 30). For the four Beaufort Sea sediments, in-depth investigation of the effects of water salinity on OSA formation was conducted at a constant sediment concentration of 200 mg/L (Figure 31).

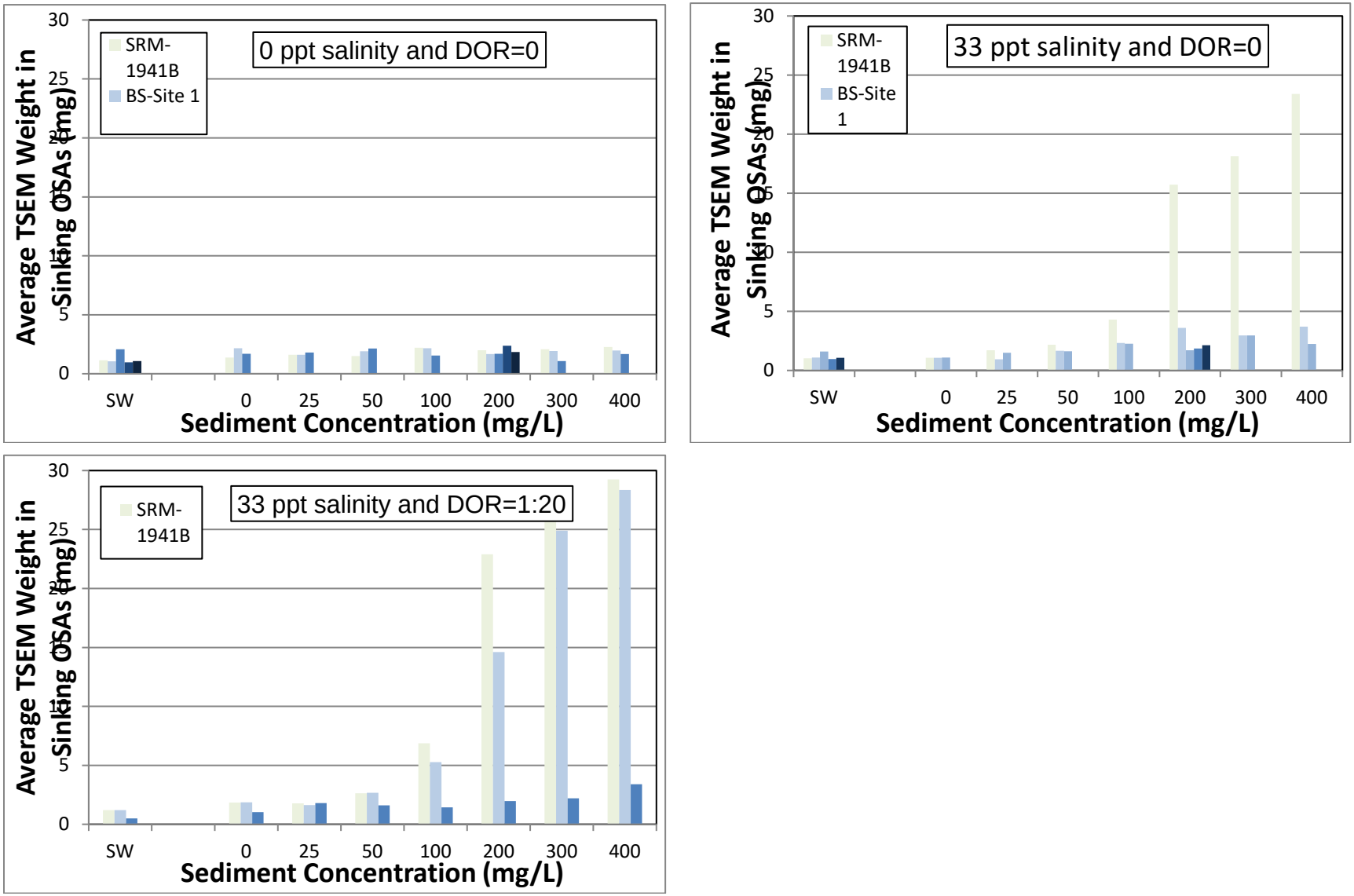

Figure 27. Measured oil sedimentation (TSEM in sinking OSAs) from experiments using Amauligak crude oil, 0 ppt water salinity and no dispersant, and 33 ppt and 1:20 DOR at a controlled water temperature of 15 ^{o}C. The scale of the vertical axis was kept constant in the three plots to facilitate visual comparison between the results obtained under the three different conditions.

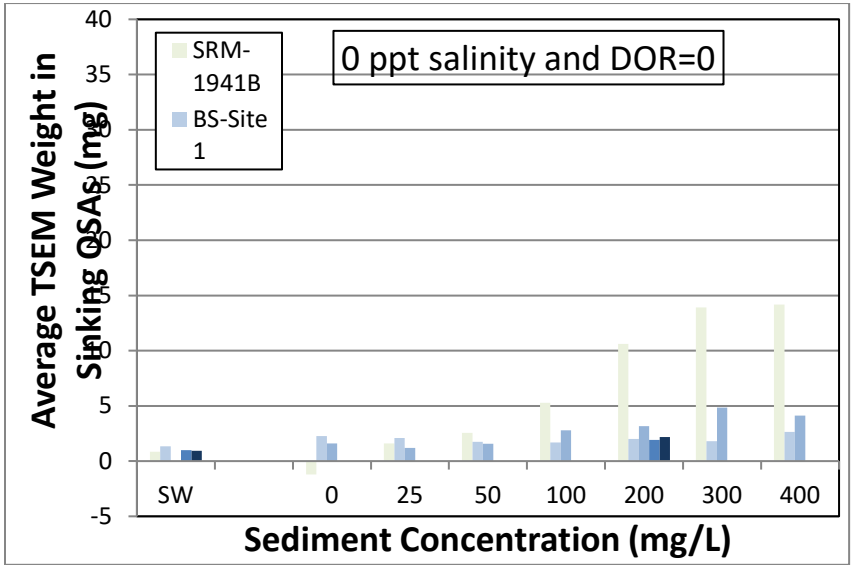

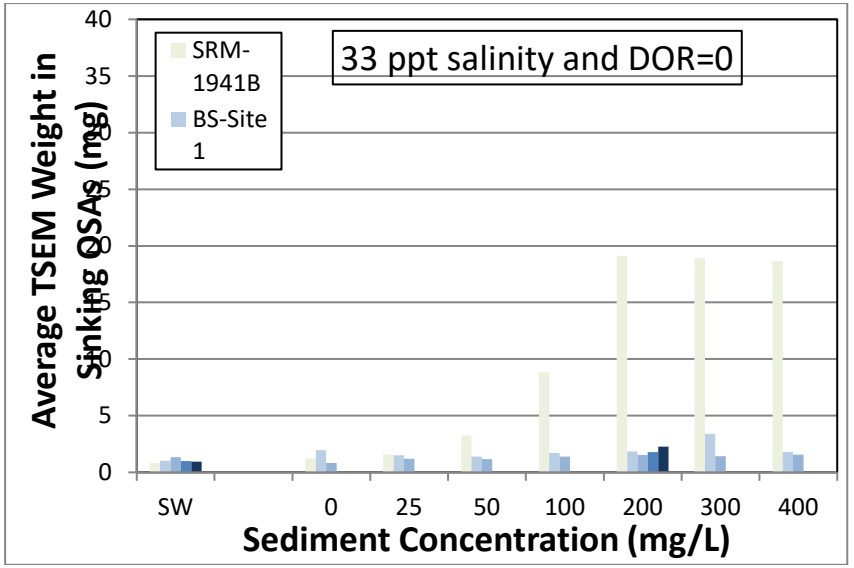

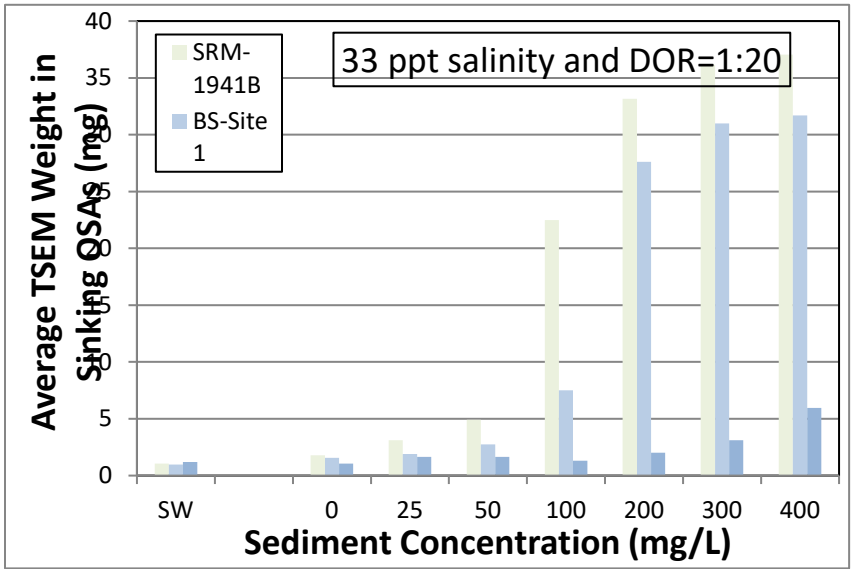

Figure 28. Measured oil sedimentation (TSEM in sinking OSAs) from experiments using Alkinson crude oil, 0 ppt water salinity and no dispersant, and 33 ppt and 1:20 DOR at a controlled water temperature of 15 ^{o}C. The scale of the vertical axis was kept constant in the three plots to facilitate visual comparison between the results obtained under the three different conditions.

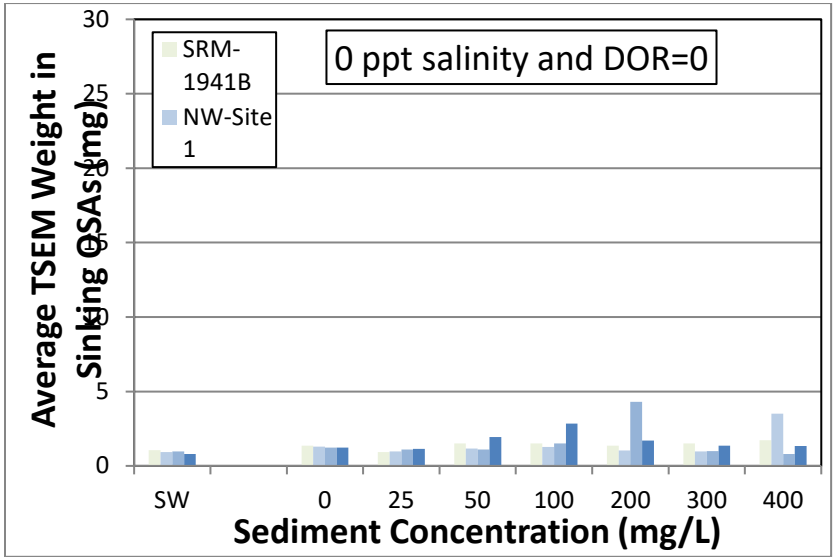

Figure 29. Measured oil sedimentation (TSEM in sinking OSAs) from experiments using Norman Wells crude oil, 0 ppt water salinity and no dispersant, and a controlled water temperature of 15 ºC. The scale of the vertical axis was kept the same as in Figure 13 to facilitate visual comparison between the results obtained under the three different conditions.

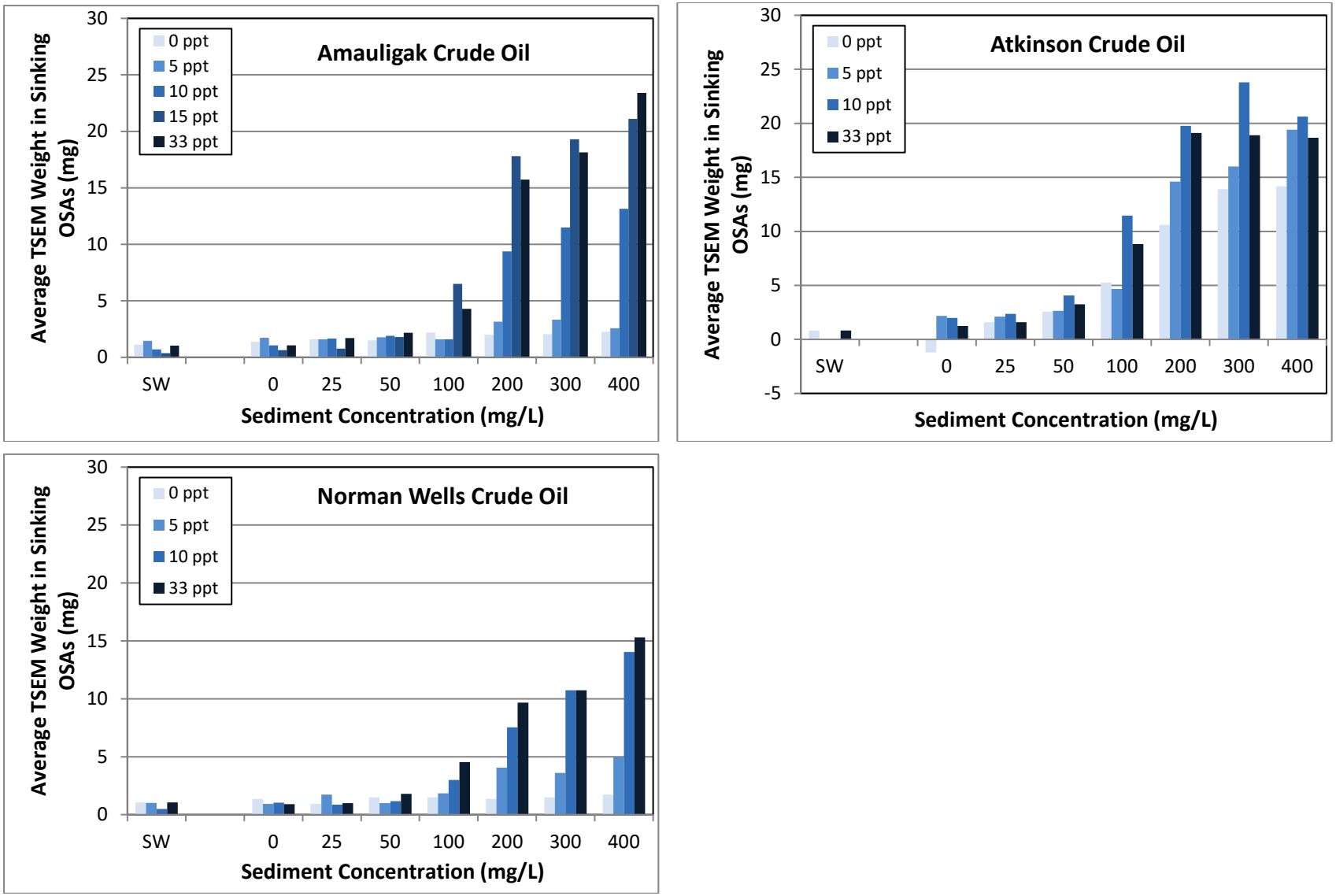

Figure 30. Measured oil sedimentation (TSEM in sinking OSAs) from experiments using the three crude oils, SRM-1941b sediment, different water salinities, controlled water temperature of 15 ^{o}C, and no dispersant. The scale of the vertical axis was kept constant in the three plots to facilitate visual comparison between the results obtained with three different crude oils.

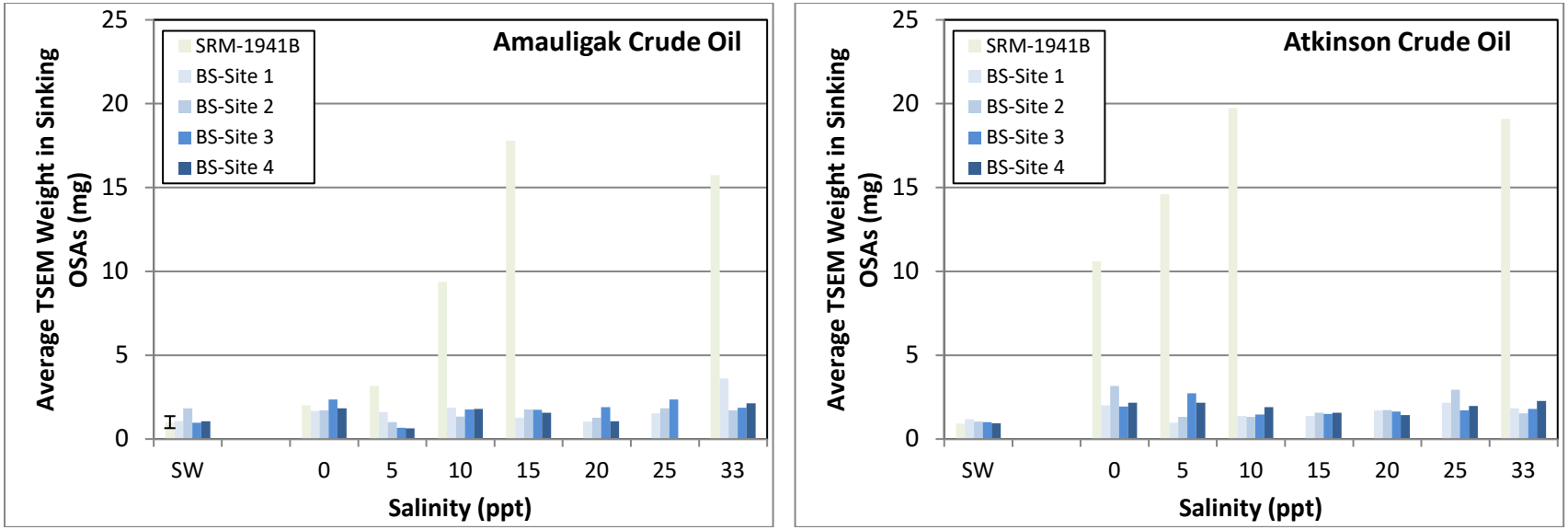

Figure 31. Measured oil sedimentation (TSEM in sinking OSAs) from experiments using the Amauligak and Atkinson crude oils, the four Beaufort Sea and the SRM-1941b sediments, different water salinities, controlled water temperature of 15 ^{o}C, constant sediment concentration of 200 mg/L, and no dispersant.

5.3.3. Effects of water temperature for different sediment types and concentrations.

The effects of temperature on OSA formation were studied using SRM-1941b sediment and the three Arctic crudes oils. A series of experiments were performed using variable sediment concentrations at both 15 ºC and freezing temperature of 0 ºC. Two representative salinities of the Mackenzie River Delta of 5 (Figure 32) and 33 ppt (Figure 33) were used.

5.3.4. Effects of chemical dispersant for different sediment types and concentrations.

The effects of chemical dispersant on OSA formation were studied using SRM-1941b sediment and the three Arctic crudes oils. Series of experiments were performed using variable sediment concentrations at both 15 ºC and freezing temperature of 0 ºC. All experiments were run using a constant salinity of 33 ppt. Results are shown in Figures 34 to 36.

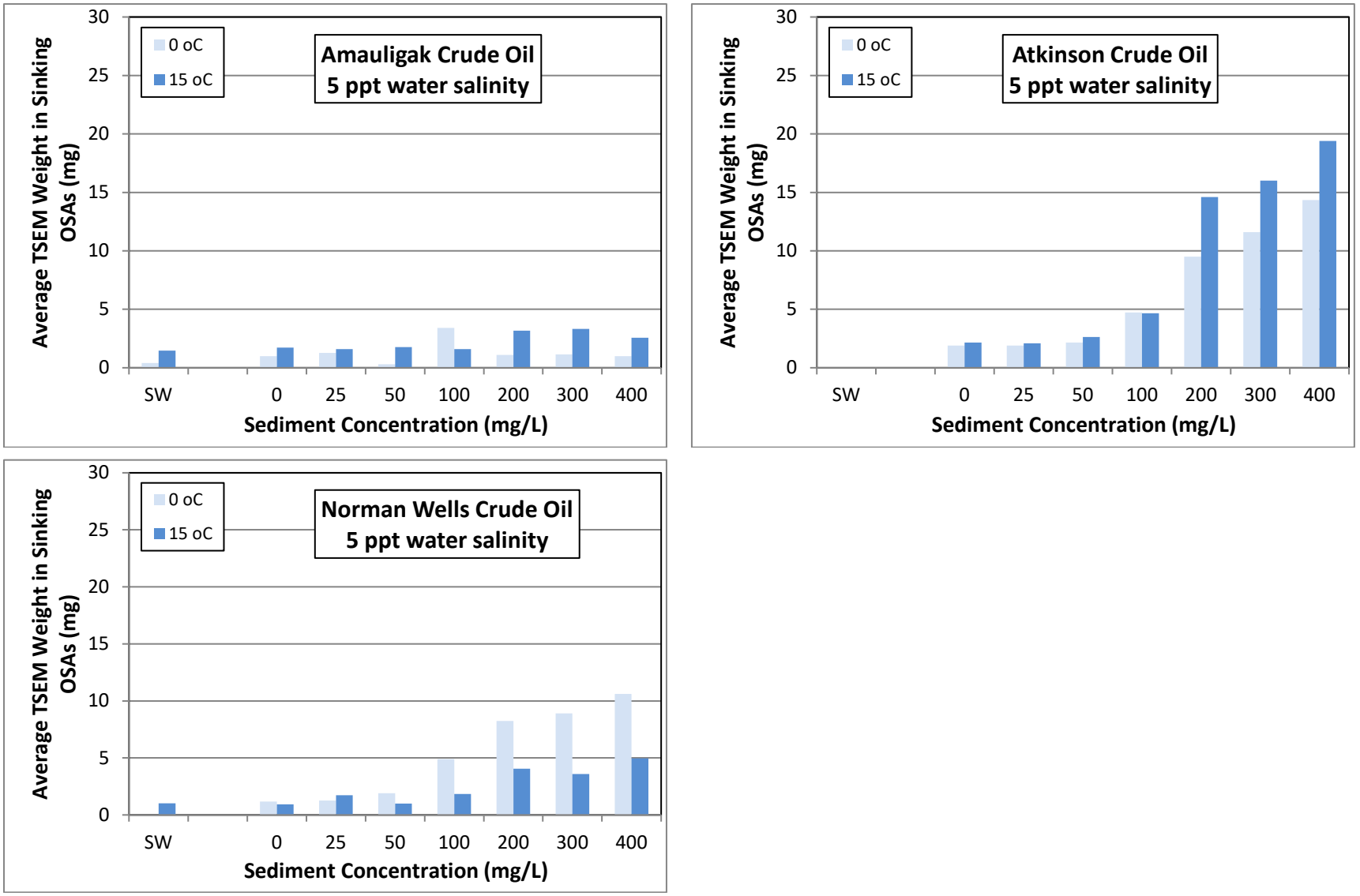

Figure 32. Measured oil sedimentation (TSEM in sinking OSAs) from experiments using the three Arctic crude oils, the SRM-1941b sediments, various sediment concentrations, 5 ppt water salinities, two different water temperature of 0 and 15 ^{o}C, and no dispersant.

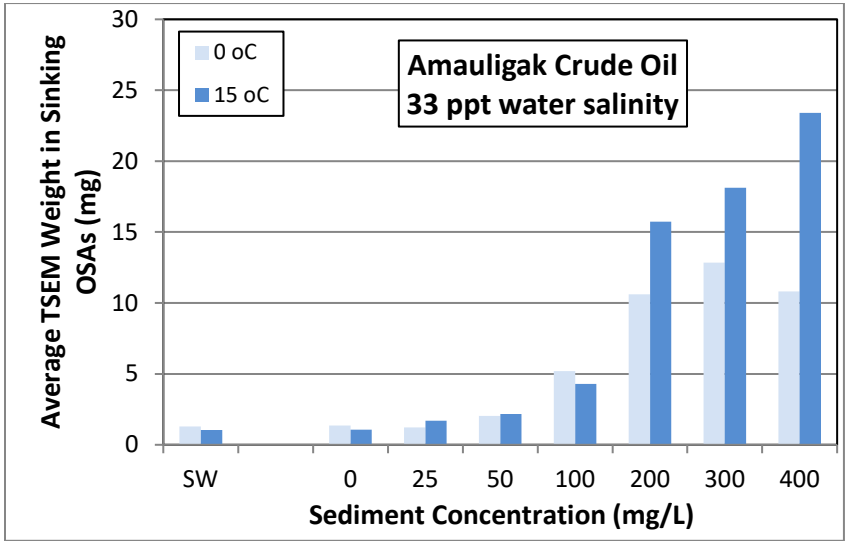

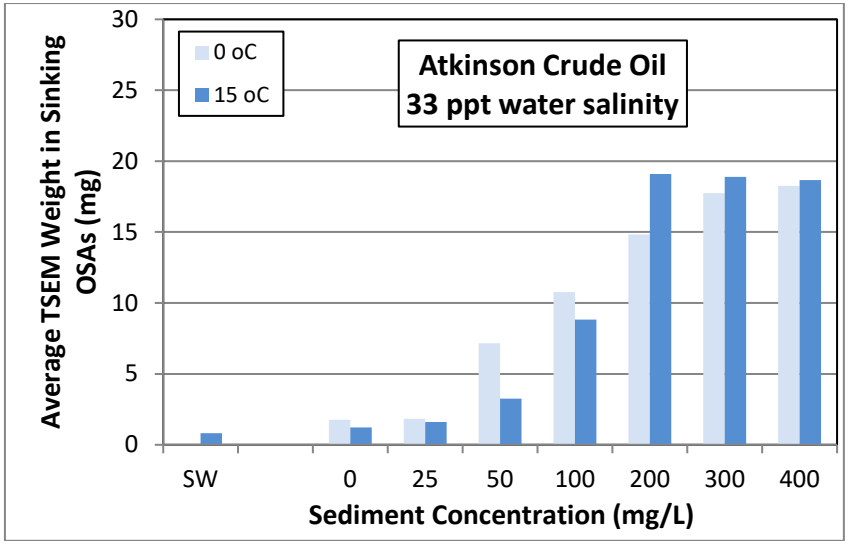

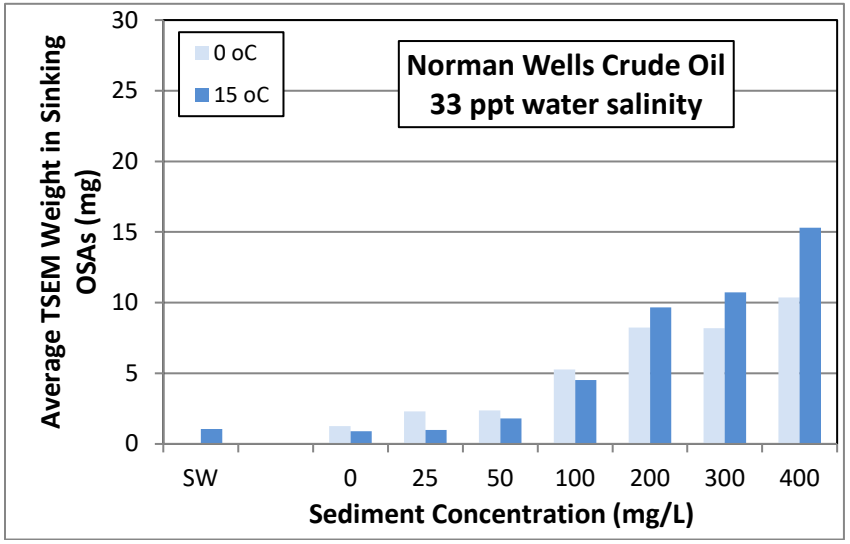

Figure 33. Measured oil sedimentation (TSEM in sinking OSAs) from experiments using the three Arctic crude oils, the SRM-1941b sediments, various sediment concentrations, 33 ppt water salinities, two different water temperature of 0 and 15 ^{o}C, and no dispersant.

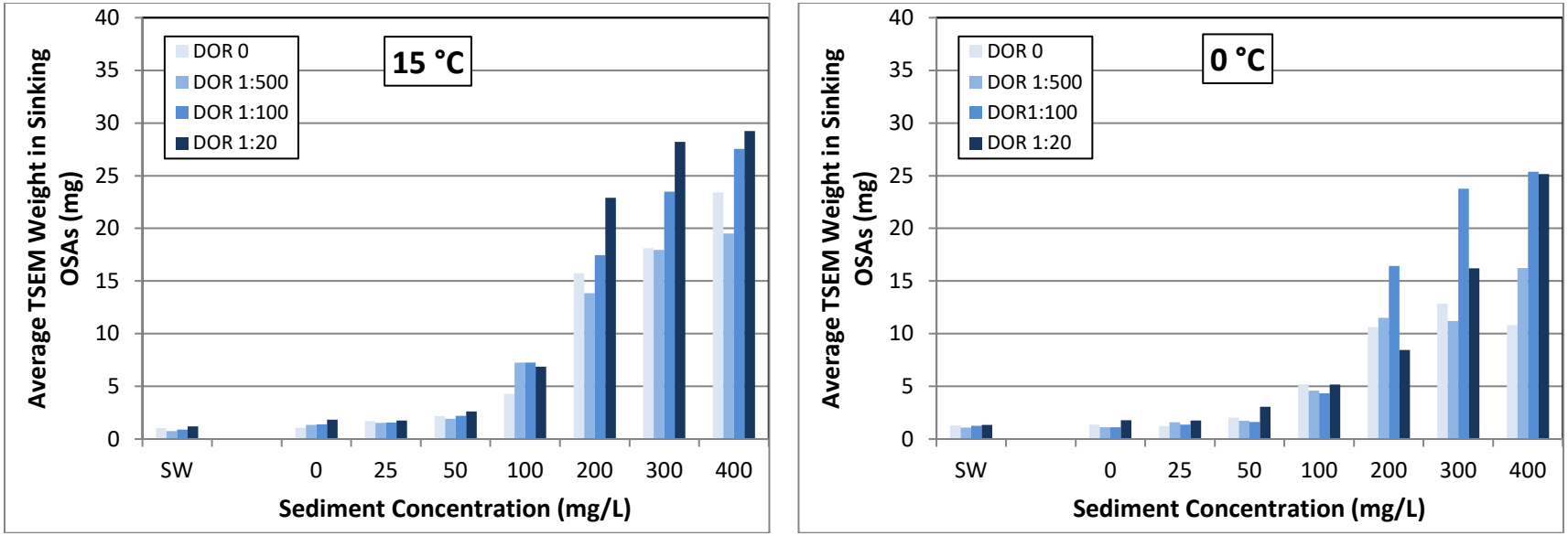

Figure 34. Measured oil sedimentation (TSEM in sinking OSAs) from experiments using Amauligak crude oil, the SRM-1941b sediments, various sediment concentrations, 33 ppt water salinities, two different water temperature of 0 and 15 ^{o}C, and various dispersant dosages (DOR).

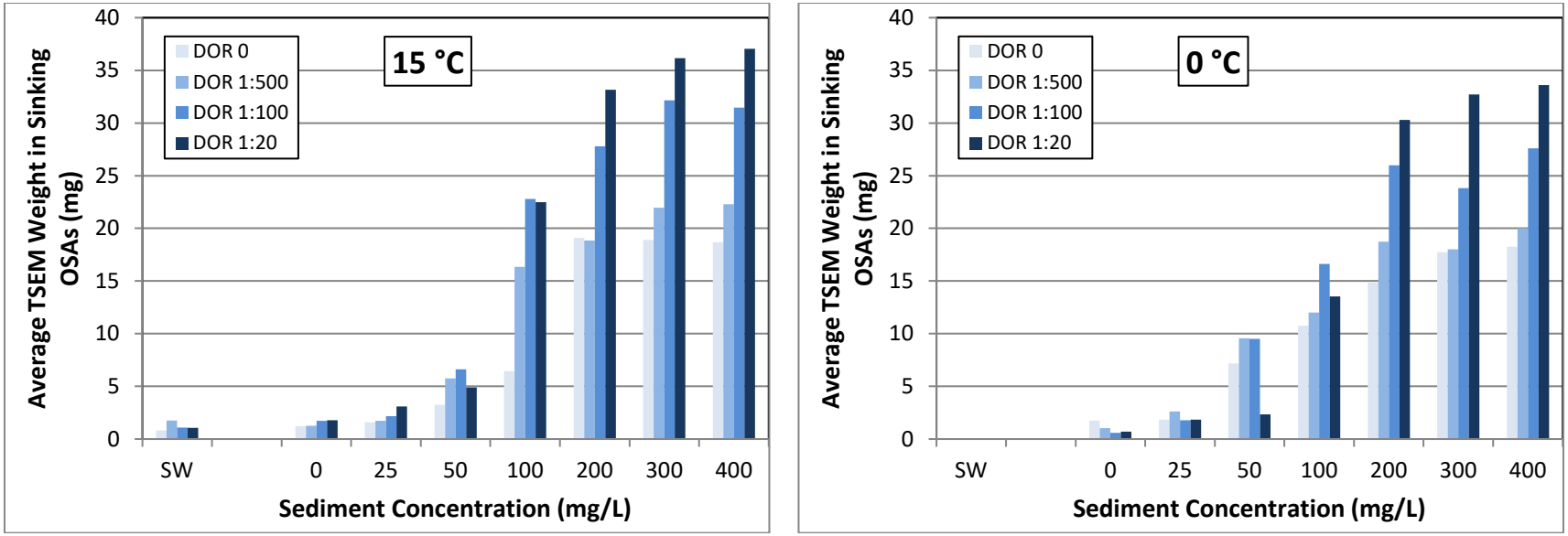

Figure 35. Measured oil sedimentation (TSEM in sinking OSAs) from experiments using Atkinson crude oil, the SRM-1941b sediments, various sediment concentrations, 33 ppt water salinities, two different water temperatures of 0 and 15 ^{o}C, and various dispersant dosages (DOR).

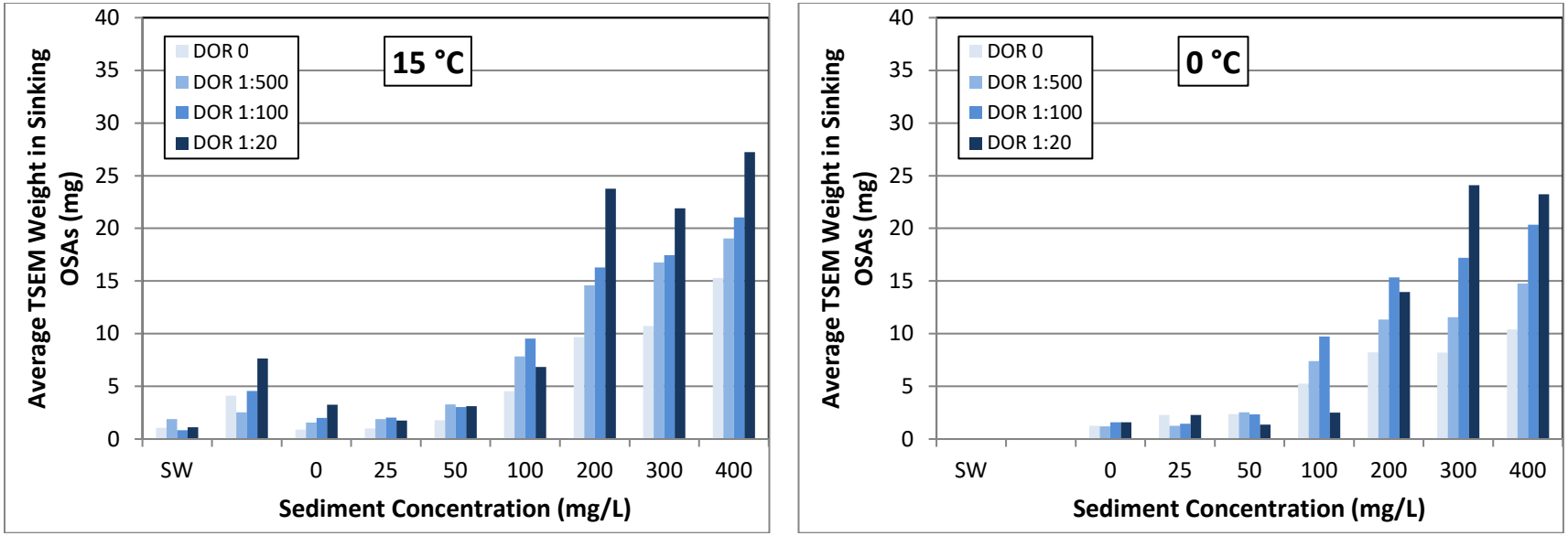

Figure 36. Measured oil sedimentation (TSEM in sinking OSAs) from experiments using Norman Wells crude oil, the SRM-1941b sediments, various sediment concentrations, 33 ppt water salinities, two different water temperatures of 0 and 15 ^{o}C, and various dispersant dosages (DOR).

5.3.5. Physical properties of OSAs formed with Arctic oils

A new state-of-the-art settling column device was developed to measure physical properties of OSAs. The setup is computer controlled and includes several parts as shown in Figure 37. The experiments on OSA settling were conducted at room temperature. The water temperature in the column was measured at the beginning of each test. The average value was 20.9 ^{o}C and the standard deviation 1.2 ^{o}C.

A constant sediment concentration of 200 mg/L was used in these experiments. Sediment samples SRM-1941b, BS-Site 1 and NW-Site 3 were used. Two DOR of 0 and 1:20 were studied. Measured settling velocity for OSAs formed with Norman Wells, Amauligak and Atkinson crude oils are shown in Figure 38 to 40. The data show that when oil is added, especially with the addition of dispersant, large flocs form. These larges flocs are expected to be OSAs. They settle as sediment flocs as shown in previous studies (Khelifa et al, 2008). Their settling velocity is around 1 mm/s. However, the data showed that OSAs may settle at higher or lower speed, depending on their size, their oil content and their form.

The plots of the size distribution are shown in Figures 41 to 43. In all these figures, the “OSA and/or Sediment Floc Size” (horizontal axis) refers to the equivalent diameter of the flocs measured using image analysis. The results show that when oil is added, the size distribution shifts to the larger sizes. This trend is more evident with dispersant than without.

Modified Stokes Law was used to calculate the density of the sediment and OSA flocs. The results are shown in Figures 44 to 46. As well known for sediment flocs, the data show a consistent decrease of the density of the flocs/OSAs with their size. Larger particles, expected to be OSAs have a low effective density of few tens of g/L

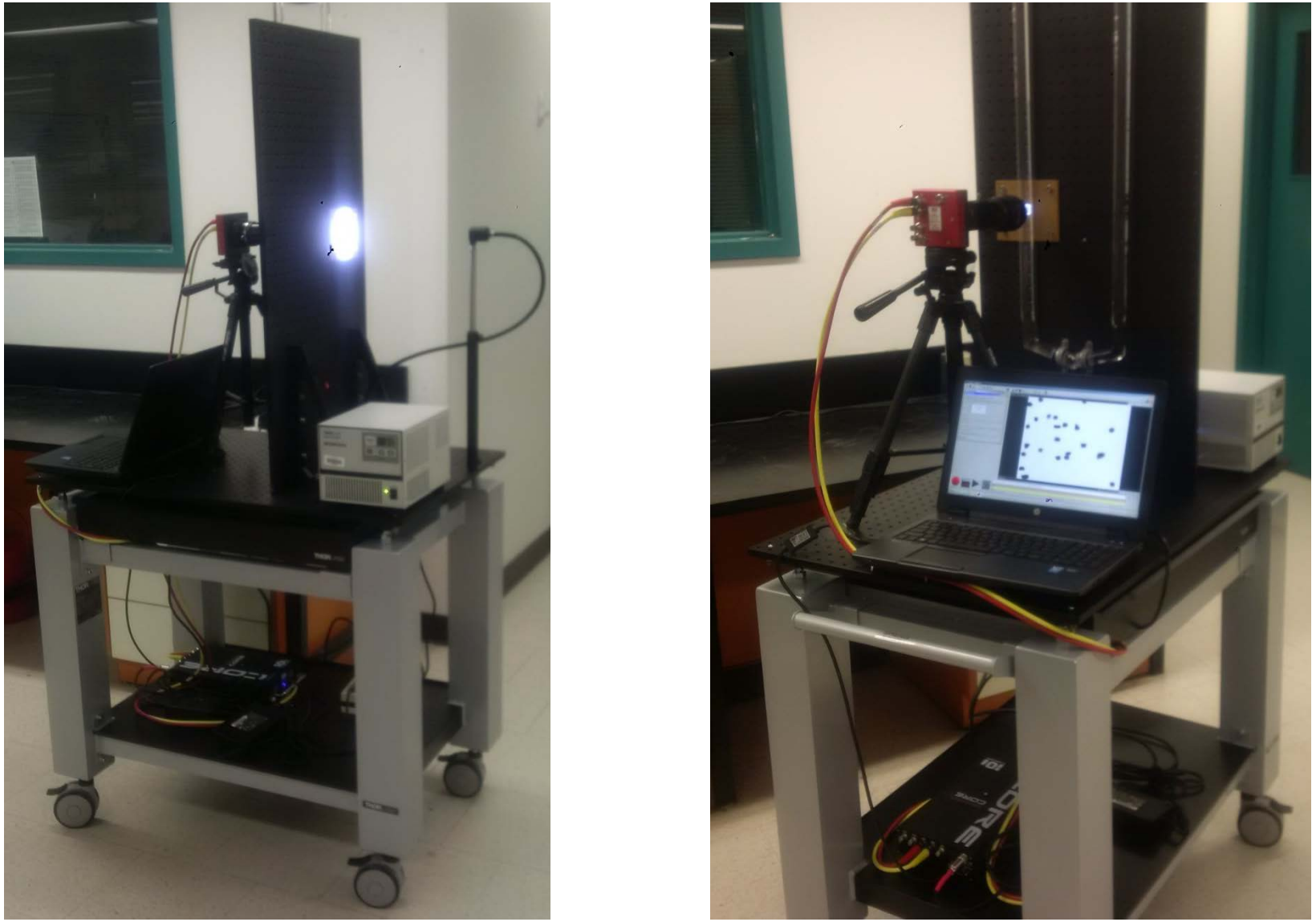

Figure 37. Pictures of the new state-of-the-art settling column developed in this project to measure physical properties of OSAs

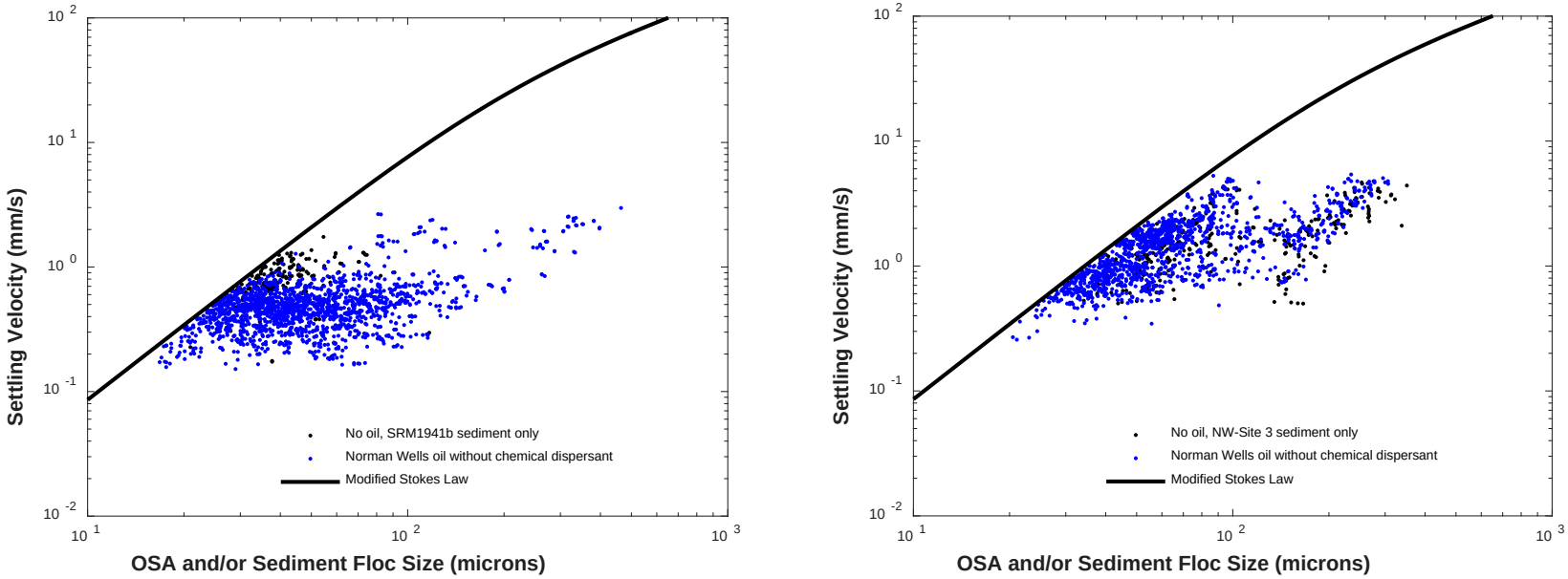

Figure 38. Measured settling velocity of sinking OSAs formed with SRM-1941b and NW-Site 3 sediments at 200 mg/L concentration and Norman Wells crude oil, at 0 ppt water salinity, without dispersant, and at room temperature of 20.9 ºC, The data are compared to those obtained without oil (sediment flocs) and without chemical dispersant (black dots).

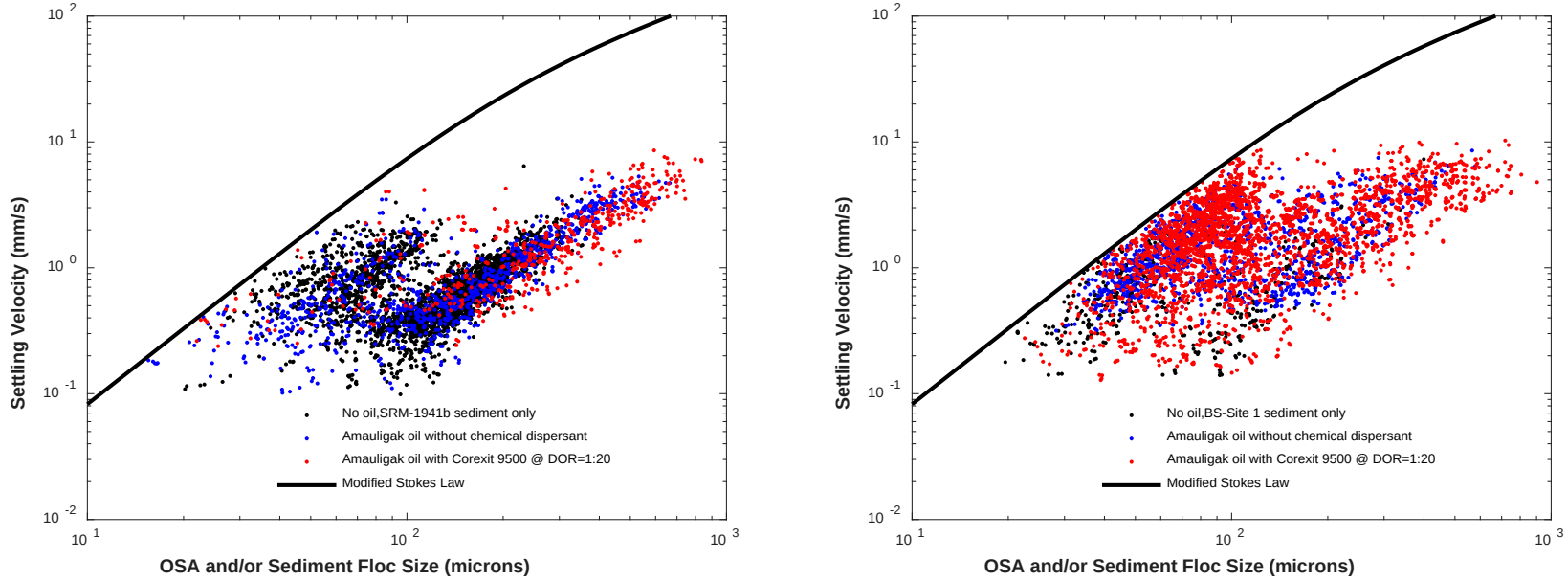

Figure 39. Measured settling velocity of sinking OSAs formed with SRM-1941b and BS-Site 1 sediments at 200 mg/L concentration and Amauligak crude oil, at 33 ppt water salinity, without and with Corexit EC9500A at 1:20 DOR, and at room temperature of 20.9 ^{o}C, The data are compared to those obtained without oil (sediment flocs) and without chemical dispersant (black dots).

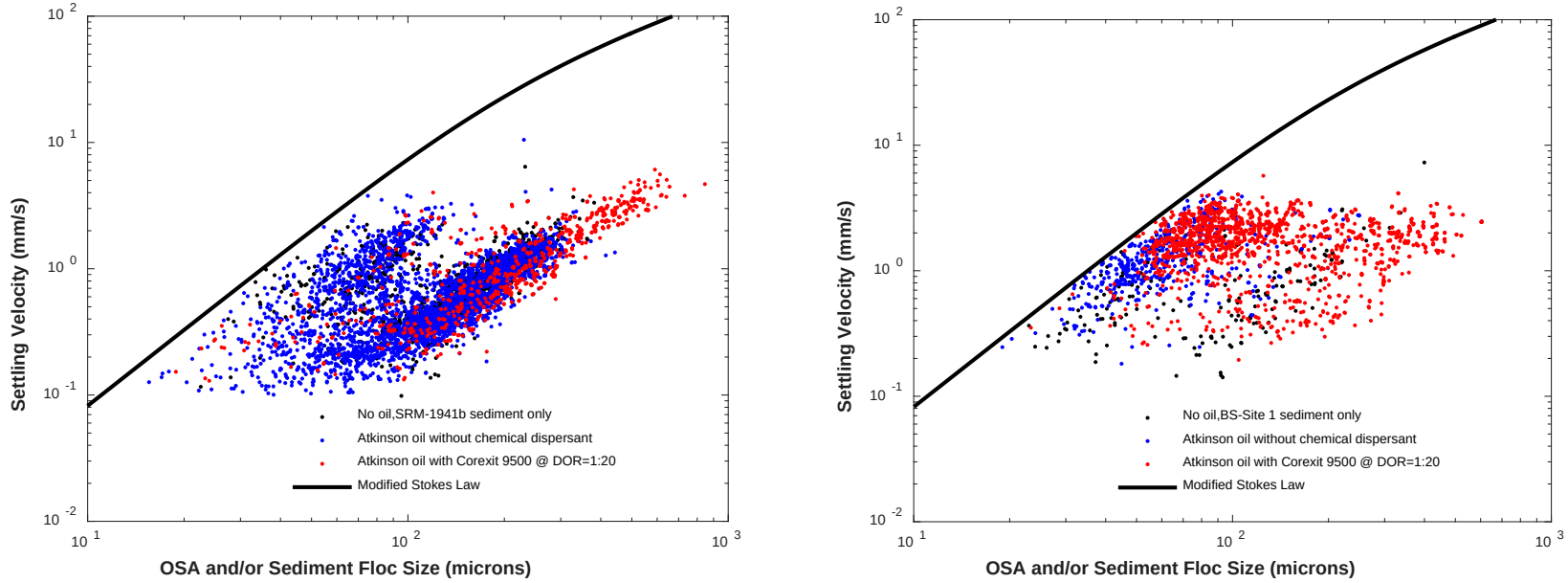

Figure 40. Measured settling velocity of sinking OSAs formed with SRM-1941b and BS-Site 1 sediments at 200 mg/L concentration and Atkinson crude oil, at 33 ppt water salinity, without and with Corexit EC9500A at 1:20 DOR, and at room temperature of 20.9 ^{o}C, The data are compared to those obtained without oil (sediment flocs) and without chemical dispersant (black dots).

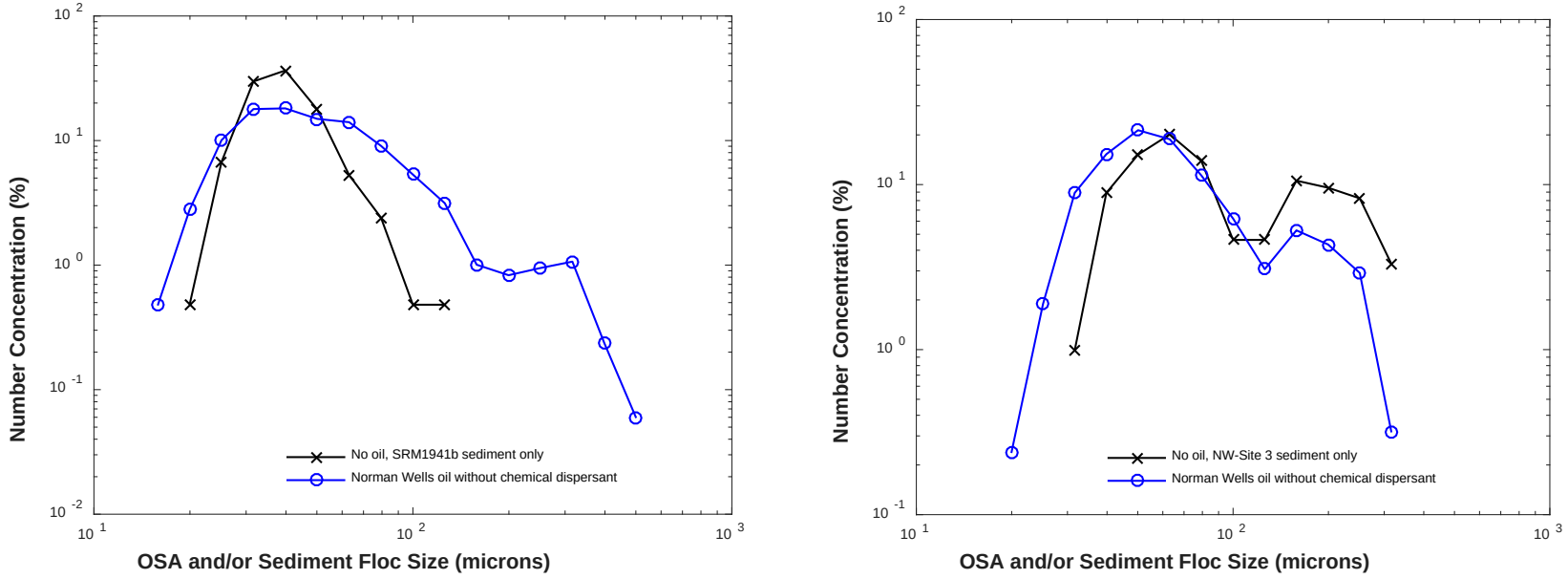

Figure 41. Measured size distribution of sinking OSAs formed SRM-1941b and NW-Site 3 sediments at 200 mg/L concentration and the Norman Wells crude oil, at 0 ppt water salinity, without dispersant, and at room temperature of 20.9 ^{o}C, The data are compared to those obtained without oil (sediment flocs) and without chemical dispersant (black dots).

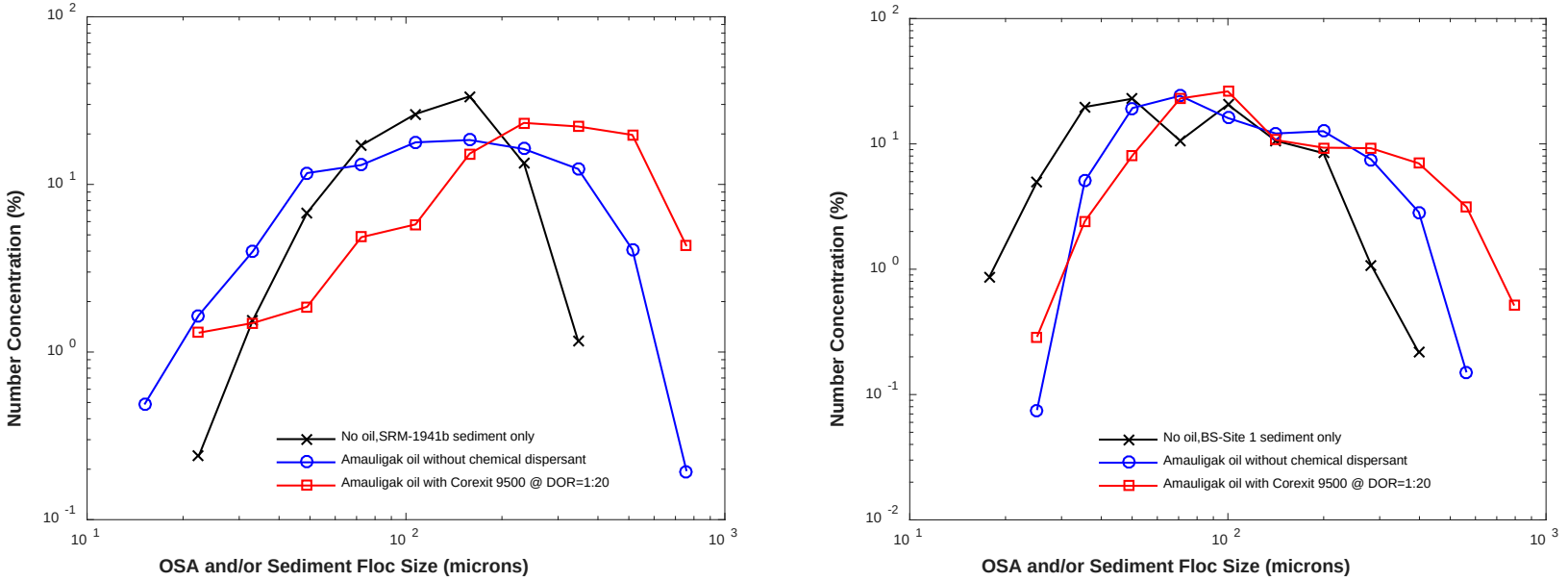

Figure 42. Measured size distribution of sinking OSAs formed SRM-1941b and BS-Site 1 sediments at 200 mg/L concentration and Amauligak crude oil, at 33 ppt water salinity, without and with Corexit EC9500A at 1:20 DOR, and at room temperature of 20.9 ^{o}C, The data are compared to those obtained without oil (sediment flocs) and without chemical dispersant (black dots).

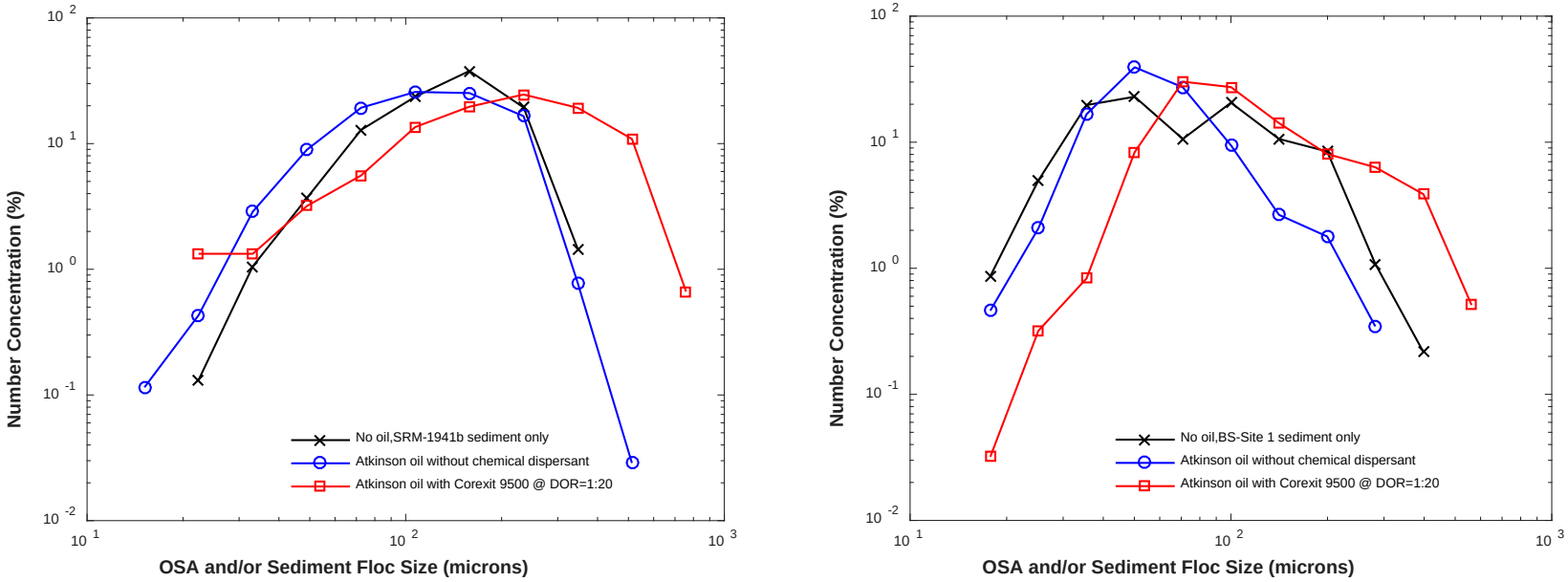

Figure 43. Measured size distribution of sinking OSAs formed SRM-1941b and BS-Site 1 sediments at 200 mg/L concentration and Atkinson crude oil, at 33 ppt water salinity, without and with Corexit EC9500A at 1:20 DOR, and at room temperature of 20.9 ^{o}C, The data are compared to those obtained without oil (sediment flocs) and without chemical dispersant (black dots).

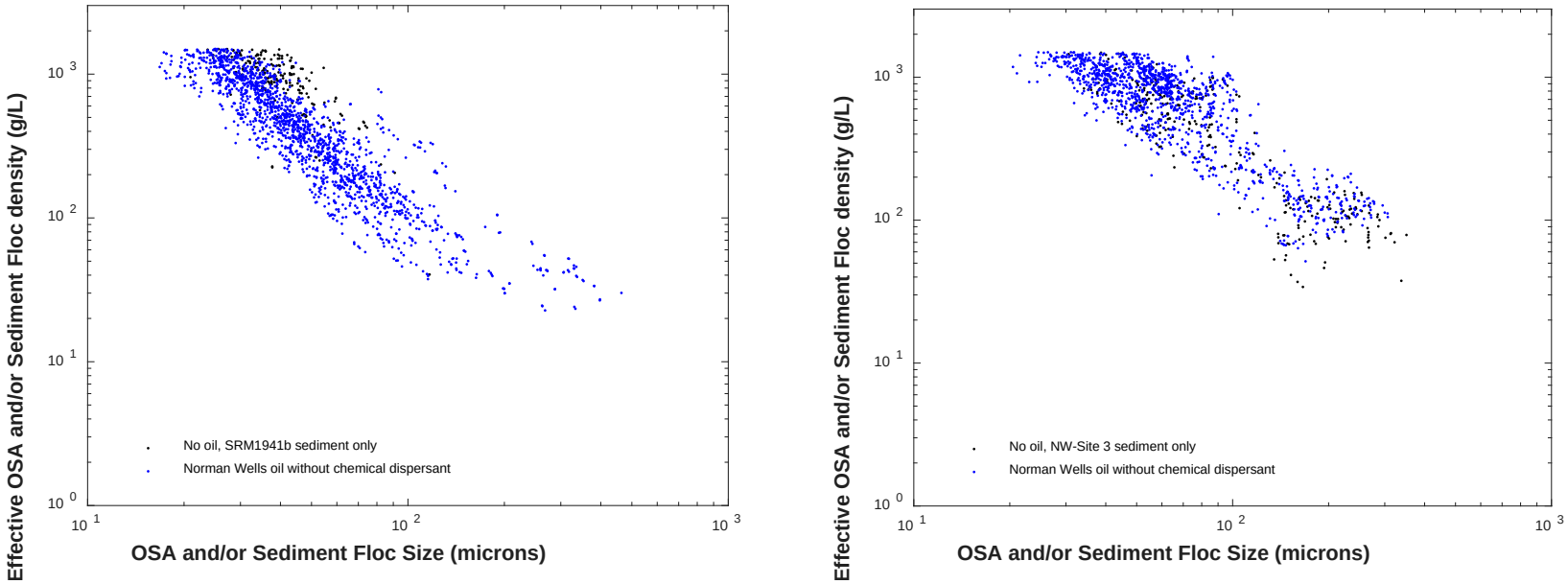

Figure 44. Measured effective density of sinking OSAs formed SRM-1941b and NW-Site 3 sediments at 200 mg/L concentration and the Norman Wells crude oil, at 0 ppt water salinity, without dispersant, and at room temperature of 20.9 ^{o}C, The data are compared to those obtained without oil (sediment flocs) and without chemical dispersant (black dots).

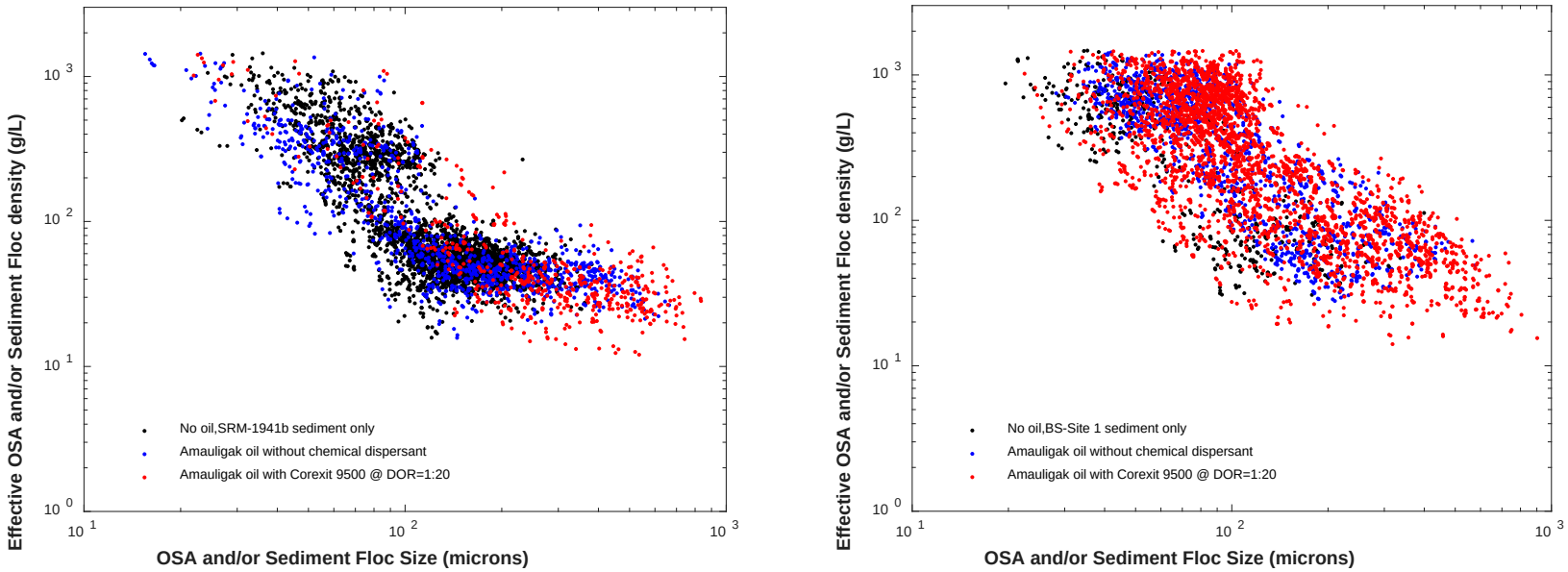

Figure 45. Measured effective density of sinking OSAs formed SRM-1941b and BS-Site 1 sediments at 200 mg/L concentration and Amauligak crude oil, at 33 ppt water salinity, without and with Corexit EC9500A at 1:20 DOR, and at room temperature of 20.9 ^{o}C, The data are compared to those obtained without oil (sediment flocs) and without chemical dispersant (black dots).

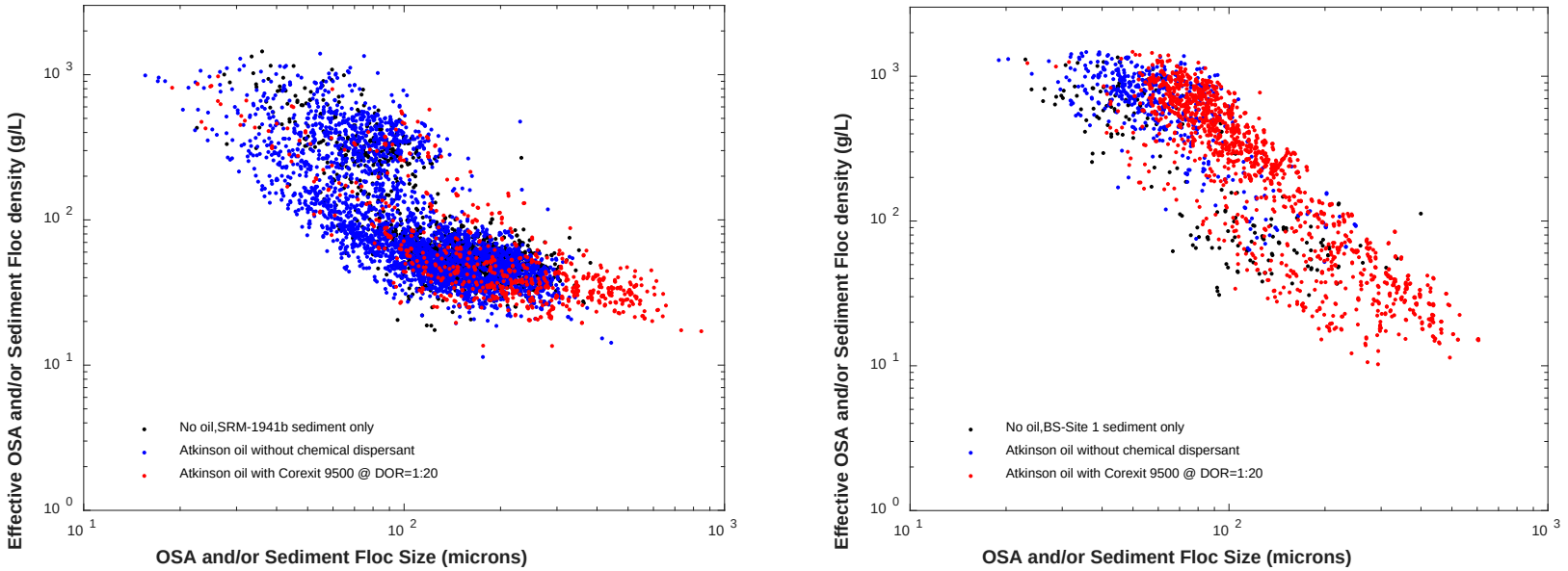

Figure 46. Measured effective density of sinking OSAs formed SRM-1941b and BS-Site 1 sediments at 200 mg/L concentration and Atkinson crude oil, at 33 ppt water salinity, without and with Corexit EC9500A at 1:20 DOR, and at room temperature of 20.9 ^{o}C, The data are compared to those obtained without oil (sediment flocs) and without chemical dispersant (black dots).

6. Data analysis and discussion

6.1. Oil dispersion

IFT measured with brine is smaller than freshwater (Figure 13). But, the effect of salinity on IFT reduction was not high when dispersant was not applied. The maximum reduction measured with Amauligak crude oil was less than 1 mN/m. The reduction of IFT with water temperature is slightly higher than with water salinity (Figure 12). This will cause some enhancement of natural oil dispersion at higher temperatures. This is on the top of the enhancement caused by the reduction of oil viscosity when the temperature is increased.

The reduction of IFT measured when Corexit EC9500A (chemical dispersant) was applied is much higher than the reductions caused by water salinity and/or temperature (Figures 14 and 15). A small DOR of 1:500 causes a reduction of the IFT of Amauligak crude oil by about 18 mN/m (IFT decreases from 22.3 to 3.6 mN/m)! A similar result was found for Norman Wells crude oil, as validated by the measured size distributions of dispersed oil droplets (Figure 18-20). It is also interesting to note that the reduction of IFT of Amuligak with DOR followed almost the same trend and intensity for both 5 and 33 ppt water salinities (Figures 14 and 15). The data obtained with Atkinson are consistent with this trend, but the reduction of IFT and the formation of oil droplet at low DOR are not as significant as for the other two crudes. The data is presented in Figure 21. Among the three crudes, Norman Wells appears to be the more dispersible, followed by Amauligak and then Atkinson. This is not consistent with the results obtained at a DOR of 1:500 in Figure 21. But, a closer look at the results shows that the trend shown in that plot is just an artifact of the way the data were processed. The reason why Atkinson appears to form more small droplets than the other two oils at DOR 1:500 (Figure 21) relates to the fact that far fewer droplets are formed with Atkinson and the total number of the dispersed droplets, with which the data were normalized, is much less than the corresponding ones obtained with the other oils. A clear illustration of this is shown in Figure 22. The scale of the three images is the same.

Quantitative results shown in Figures 12 to 15 regarding IFT reductions and in 18-21 regarding droplet size distribution are fundamental for modelling spill of these oils and the development of fundamental behaviour model of the dispersion of these oils.

6.2. OSA formation

In this section all references to OSAs relates to negatively buoyant OSAs.

Very few OSAs were formed in freshwater with Amauligak and Atkinson crudes and the four BS sediments (Figures 27 and 28), and with Norman Wells crude and the three NW sediments (Figure 29). Interestingly, a significant amount of OSAs formed with Atkinson and the SRM-1941b sediment with freshwater. About 20 % and 28% of the oil was trapped in the OSAs at sediment concentrations of 200 mg/L and 300 mg/L, respectively. The superiority of Atkinson crude to form OSA appears to be linked to its relatively high asphaltene content compared to Amauligak and Norman Wells crudes (Table 1). It has been shown that OSA formation increases with asphalthene content (Khelifa et al., 2002)

Very high amounts of OSA formed with Amauligak and Atkinson crudes and the SRM-1941b sediment in saltwater. However, very few OSAs formed with BS sediments in saltwater.

Application of Corexit EC9500A at 1:20 DOR boosted OSA formation with both Amauligak and Atkinson crude and SRM-1941b and BS-Site 1 sediments (Figures 27 and 28). Very small amounts of OSA formed with the other sediments samples. The fundamental reason for this behaviour relates to the high organic matter content (Table 4) and fine content (sediment grains up to 5 μm in size) (Table 5 and Figure 10) in the sediment samples. The organic matter content for SRM-1941b was measured to be 10.6 % in weight (Khelifa al., 2008). This is consistent with the state-of-knowledge (Khelifa et al., 2008, Gong et al., 2014)

More in-depth testing of OSA formation with the three oils at different water salinity showed that OSAs form readily with the three crudes and the SRM-1941b sediment and water salinity has a strong impact on the process (Figure 30). The four BS sediments form very few OSAs at all water salinities. While this may be attributed primarily to the low fine content in most of these sediment samples (Table 5), it is not clear why the BS-Sites with a relatively high fine content did not form OSA at high salinities when Corexit EC9500A was not applied.

Investigation on the effects of temperature on OSA formation using SRM-1941b sediment revealed that the interaction continues to occur at freezing temperature of 0 ^{o}C with Atkinson crude at 5 ppt water salinity (Figure 32). For Norman Wells crude, the results show that more OSA formed at 0 ^{o}C than at 15 ^{o}C. This is an interesting trend that calls for further investigation to better understand and

quantify such unexpected behaviour. At 33 ppt, the three crudes form a significant amount of OSA at 0 ^{o}C (Figure 33).

Further investigation of the effect of temperature on OSA formation with SRM-1941b sediment was conducted with Corexit EC9500A (Figures 34-36). Results show that a significant amount of OSAs will readily form at 0 ^{o}C with the three crudes at any DOR and sediment concentration of 100 mg/L and higher. At a 50 mg/L concentration of SRM-1941b sediment, 10 % of the Atkinson crude is associated with OSAs at 0 ^{o}C.

Results shown in Figures 34 to 36 demonstrate that application of Corexit EC9500A significantly enhances the formation of negatively buoyant OSAs and related oil sedimentation. This is consistent with the findings from previous studies using different natural sediments and different crudes (Khelifa et al, 2008). Application of chemical dispersant does not prevent sediment fines from aggregating with chemically dispersed oil droplets to form OSAs. This study has shown that these findings apply to OSA formation under freezing temperatures as well.

Another important finding illustrated in Figures 34 to 36 is that the addition of small amounts of Corexit EC9500A at DOR of 1:500 can significantly enhance OSA formation.

The results obtained with settling column devise show that when oil is added, the size distribution of OSA and/or sediment flocs shifts to the larger sizes (Figures 41 to 43). This trend is more evident with dispersant than without. This is illustrated further in Figure 47 showing images of OSA and/or sediment flocs when falling in the settling column. This suggests that OSAs are more resistant to shear and mixing than sediment flocs, which show that sediment fines are strongly bonded to the oil droplets. This is also consistent with the findings of previous studies (Khelifa et al., 2008).

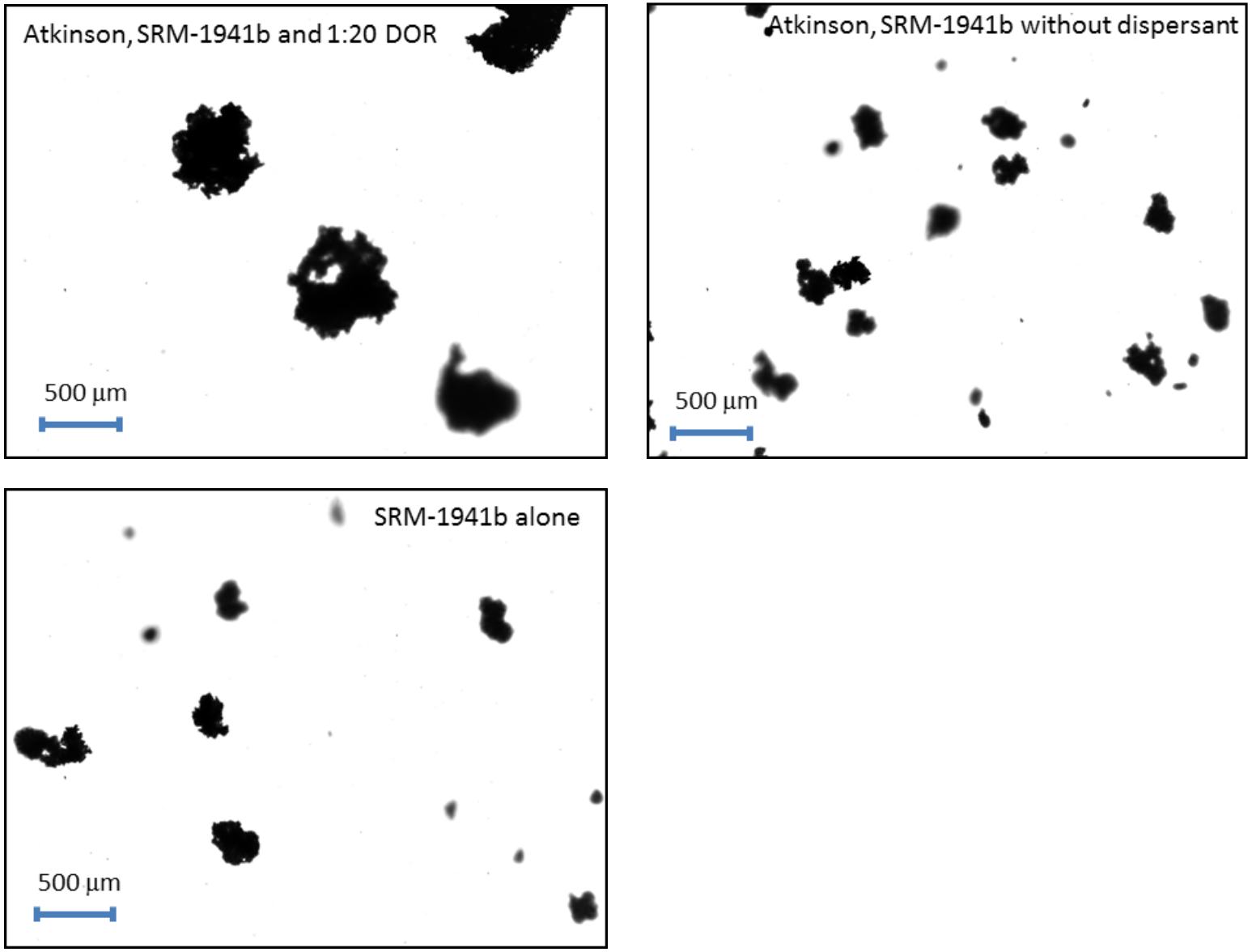

Figure 47. Typical images of sediment and/or OSA flocs settling in the settling column devise. Test with Atkinson crude, SRM-1941b sediment at 200 mg/L concentration and 33 ppt water salinity.

7. Conclusions

Key conclusions from this study are:

1. Amauligak, Atkinson and Norman Wells crude oils do not disperse at a moderate mixing energy quantified by a 2.3 Hz orbital rotation speed of the shaker used in this study. Under the same mixing energy, the addition of a small concentration of Corexit EC9500A with DOR of 1:500 was sufficient to disperse the oils. This is attributed to the significant reduction in the IFT.
2. Significant quantitative information regarding IFT reduction and dispersed oil droplets with different DORs was generated in this project and presented in this report. This is key information for modelling spills of these oils,
3. With the very kind support of Brian Yurris from Water Survey of Canada of Environment and Climate Change Canada and Dustin Whalen from Geological Survey of Canada of Natural Resources Canada several sediment samples from Norman Wells, NWT and the Mackenzie River Delta in the Beaufort Sea were obtained in this project and saved for future research on oil-sediment interaction in these water systems. These sediment samples required extensive efforts to obtain.
4. The three subject oils formed OSAs readily with SRM-1941 sediment at both 15 ^{o}C and freezing temperature of 0 ^{o}C when sediment concentration is 100 mg/ or higher.
5. Water salinity has strong impact on OSA formation when it increases from 0 to about 10ppt, but had less impact at higher salinities.
6. Application of Corexit EC9500A enhances OSA formation significantly at both 15 ^{o}C and freezing temperature of 0 ^{o}C. A small dosage of Corexit EC9500A of 1:500 is sufficient to enhance OSA formation. This is due to two key factors: 1) Corexit EC9500A causing a significant reduction of the IFT, 2) Corexit EC9500A does not prevent sediment fines from aggregating on the surface of the chemically dispersed oil droplets.
7. Application of Corexit EC9500A appears to be efficient in dispersing the three oils at 0 ^{o}C because OSA formation increased when this dispersant was added.

8. Among the natural sediment samples used in this study, BS-Site 1 with high fine content appears to be the best candidate to form OSAs.
9. This study confirms that fine content is a controlling factor in OSA formation.
10. Physical properties of OSAs are similar to those of sediment flocs. The presence of oil droplets in OSA structure enhances resistance to shear forces due to the strong bonding between sediment fines and the oil droplets.

8. References

Gong Y., Zhao X., Cai Z., O'Reilly S.E., and 2 other authors. 2014. A Review of Oil, Dispersed Oil and Sediment Interactions in the Aquatic Environment: Influence on the Fate, Transport and Remediation of Oil Spills. *Marine Pollution Bulletin*. 79: 16-33.

Hoogsteen M.J.J, Lantinga, E.A., Bakker, E.J., Groot, C.J., and Tittonell, P.A., (2015). Estimating soil organic carbon through loss on ignition: effects of ignition conditions and structural water loss. European Journal of Soil Science, Vol. 66, pp. 320-328.

Khelifa A., Hill P.S., and Lee K. 2005a. The Role of Oil-Sediment Aggregation in Dispersion and Biodegradation of Spilled Oil. *Oil Pollution and its Environmental Impact in the Arabian Gulf Region*. A. Al-Azab, W. El-Shorbagy, and S. Al-Ghais (eds.), Elsevier, Amsterdam. 131-145.

Khelifa A., Fingas M.F., and Brown C.E. 2008. Effects of Dispersants on Oil-SPM Aggregation and Fate in U.S. Coastal Waters. *Final Report submitted to the Coastal Response Research Center*. University of New Hampshire, Project No. 06-090. 1-57.

Khelifa A., Ajijolaiya L.O., MacPherson P., Lee K., and 3 other authors. 2005b. Validation of OMA Formation in Cold Brackish and Sea Waters. *Proceedings of the Twenty-eighth Arctic and Marine Oilspill Program (AMOP) Technical Seminar*, Environment Canada, Ottawa, ON, Canada, 1:527-538.

Khelifa, A., P. Stoffyn-Egli, P.S. Hill, and K. Lee. 2002. Characteristics of Oil Droplets Stabilized by Mineral Particles: the Effect of oil Types and Temperature. Spill Science & Technology Bulletin, 8 (1):19-30.

Sun J. and Zheng X. 2009. A Review of Oil-Suspended Particulate Matter Aggregation – A Natural Process of Cleansing Spilled Oil in the Aquatic Environment. *Journal of Environmental Monitoring*. 11: 1801-1809.

Weise, A.M., C. Nalewajko, and K. Lee. 1999. Oil-Mineral Fine Interactions Facilitate Oil Biodegradation in Seawater. Environmental Technology, 20:811-824.